

(NASA-CR-136070) GRADIENT ESTIMATES FROM  
STEREO MEASUREMENTS FOR A MARTIAN VEHICLE  
M.S. Thesis (Rensselaer Polytechnic Inst.)  
70 p HC \$5.50 CSCL 14B

N74-11286

Unclas

G3/14 15491

R.P.I. TECHNICAL REPORT MP-32

GRADIENT ESTIMATES FROM STEREO MEASUREMENTS  
FOR A MARTIAN VEHICLE

by

William J. Pfeifer

National Aeronautics and Space  
Administration

Grant NGL 33-018-091

A project submitted to the Graduate  
Faculty of Rensselaer Polytechnic Institute  
in partial fulfillment of the  
requirements for the degree of

MASTER OF ENGINEERING

School of Engineering  
Rensselaer Polytechnic Institute  
May, 1973

# TABLE OF CONTENTS

	Page
LIST OF FIGURES . . . . .	v-vi
LIST OF SYMBOLS . . . . .	vi-ix
ACKNOWLEDGEMENT . . . . .	x
ABSTRACT . . . . .	xi
1. INTRODUCTION . . . . .	1
2. METHOD OF APPROACH . . . . .	2
A. Transformation of Coordinate Systems . . . . .	2
1. Stereo Angles . . . . .	2
2. Stereo Range . . . . .	4
3. Non-stereo . . . . .	6
B. Determinations of Slopes and Gradients . . . . .	6
3. ESTIMATION OF SLOPES AND THEIR COVARIANCES . . . . .	9
A. Least Square Estimate of the Slopes . . . . .	9
B. Perturbation of the Variables . . . . .	9
1. Stereo Angles . . . . .	10
2. Stereo Range . . . . .	10
C. The Covariance Matrix of the Variables . . . . .	12
1. Stereo Angles . . . . .	12
2. Stereo Range . . . . .	12
D. Covariance Matrix of the Slopes . . . . .	13
E. Variance of the Gradient . . . . .	14
F. Determination of the Gradient . . . . .	16
4. DISCUSSION OF NUMERICAL RESULTS . . . . .	16
A. Stereo Angles System . . . . .	17
B. Stereo Range System . . . . .	23

	Page
C. Comparisons of Four Point Fit with Three Point Fit ..	32
D. Standard Deviations in Vehicle System Coordinate Estimates ( $h'$ , $a'$ , $b'$ ) . . . . .	37
5. CONCLUSIONS . . . . .	50
6. REFERENCES . . . . .	53

#### APPENDIX

A. Derivation of the Perturbation Equations . . . . .	54
B. Derivation of the Covariance Matrix of the Variables	56
C. Derivation of the Slope Covariances . . . . .	57

## LIST OF FIGURES

	Page
Figure 1    Stereo Angles System Coordinates . . . . .	3
Figure 2    Stereo Range System Coordinates . . . . .	5
Figure 3    Non-stereo System Coordinates . . . . .	7
Figure 4    Relative In-Path Slopes . . . . .	18
Figure 5    Stereo Angles System: Standard Deviation in Gradient Versus Distance from Vehicle on Flat Terrain with Relative Slope = 0° . . . . .	20
Figure 6    Stereo Angles System: Standard Deviation in Gradient Versus Relative In-Path Slope for Terrain at 4 m with Data Point Spacing = 0.6 m . . . . .	22
Figure 7    Stereo Angles System: Standard Deviation in Gradient Versus Relative In-Path Slope for Terrain at 20 m with Data Point Spacing = 1.2 m . . . . .	24
Figure 8    Stereo Angles System: Standard Deviation in Gradient Versus Relative Cross-Path Slope for Terrain at 4 and 20 Meters . . . . .	25
Figure 9    Stereo Range System: Standard Deviation in Gradient Versus Terrain Distance from Vehicle with Relative Slope = 0° . . . . .	27
Figure 10   Stereo Range System: Standard Deviation in Gradient Versus Relative In-Path Slope for Terrain at 4 m with Point Spacing = 0.6 m . . . . .	29
Figure 11   Stereo Range System: Standard Deviation in Gradient Versus Relative In-Path Slope for Terrain at 20 m with Point Spacing = 1.2 m . . . . .	30
Figure 12   Stereo Range System: Standard Deviation in Gradient Versus Relative Cross-Path Slope for Terrain at 4 and 20 Meters . . . . .	31
Figure 13   Stereo Angles System: Standard Deviation in Gradient Versus Relative In-Path Slope at 4 Meters with Point Spacing = 0.6 m for 3 and 4 Point Planes . . . . .	33
Figure 14   Stereo Angles System: Standard Deviation in Gradient Versus Relative In-Path Slope at 20 Meters with Point Spacing = 1.2 m for 3 and 4 Point Planes . . . . .	34

	Page
Figure 15	Stereo Range System: Standard Deviation in Gradient Versus Relative In-Path Slope at 4 Meters with Point Spacing = 0.6m for 3 and 4 Point Planes . . . . . 35
Figure 16	Stereo Range System: Standard Deviation in Gradient Versus Relative In-Path Slope at 20 Meters with Point Spacing = 1.2m for 3 and 4 Point Planes . . . . 36
Figure 17	Stereo Angles System: Standard Deviation in Height Coordinate ( $h'$ ) Versus Distance from Vehicle for Flat Terrain with $h' = 0$ . . . . . 38
Figure 18	Stereo Angles System: Standard Deviation in Height Coordinate Versus Distance from Vehicle for Flat Terrain with $h' = 0$ . . . . . 39
Figure 19	Stereo Angles System: Standard Deviation in Coordinate $b'$ Versus Distance from Vehicle for Flat Terrain with $h' = 0$ . . . . . 40
Figure 20	Stereo Angles System: Standard Deviation in Height Coordinate Versus Distance from Vehicle for Various Values of $h'$ . . . . . 42
Figure 21	Stereo Range System: Standard Deviation in Height Coordinate Versus Distance from Vehicle for Flat Terrain with $h' = 0$ . . . . . 43
Figure 22	Stereo Range System: Standard Deviation in $a'$ and $b'$ Coordinates Versus Distance from Vehicle for Flat Terrain with $h' = 0$ . . . . . 44
Figure 23	Stereo Range System: Standard Deviation in $h'$ and $b'$ Coordinates Versus Distance from Vehicle for Various Values of $h'$ . . . . . 45
Figure 24	Non-stereo System: Standard Deviation in Height Coordinate Versus Distance from Vehicle for Flat Terrain with $h' = 0$ . . . . . 47
Figure 25	Non-stereo System: Standard Deviation in $b'$ Coordinate Versus Distance from Vehicle for Flat Terrain with $h' = 0$ . . . . . 48
Figure 26	Non-stereo System: Standard Deviation in Height Coordinate Versus Distance from Vehicle for Various Values of $h'$ . . . . . 49
Table	Comparison of Stereo and Non-stereo Measurements Using Four Point Plane Fitting . . . . . 51

# LIST OF SYMBOLS

$\alpha$	Elevation angle measured a known vertical distance from the top of the sensor mast
$\beta$	Elevation angle measured at the top of the sensor mast
$\theta$	Azimuth angle
T	Top of sensor mast
U	Terrain point
$h'$	Vertical coordinate fixed to vehicle
$a'$	Horizontal coordinate fixed to vehicle perpendicular to direction of motion
$b'$	Horizontal coordinate fixed to vehicle perpendicular to $a'$ & $h'$
L	Separation distance between transmitter and receiver (vertical)
$h$	Vertical coordinate in non-rotating system (local vertical)
$a$	Horizontal coordinate in non-rotating system perpendicular to the vehicle heading and $h$
$b$	Horizontal coordinate in non-rotating system (vehicle heading)
C	Matrix transformation for vehicle roll
$\phi$	Roll angle
B	Matrix transformation for vehicle pitch
$\xi$	Pitch angle
M	Measurement in the stereo range system
N	Measurement in the stereo range system
K	Measurement in the stereo range system
R	Range from transmitter to terrain point
P	Range from terrain point to receiver L meters below top of mast
J	Horizontal separation distance between transmitter and receiver
Q	Range from terrain point to receiver J meters from top of mast (horizontal distance=J)
$x_1$	Cross-path slope
$x_2$	In-path slope
$x_3$	Parameter in equation for plane
Sg	Gradient of terrain
$\hat{h}_i$	Height of $i^{th}$ point in modeled plane
$\bar{h}_i$	Actual measured height of $i^{th}$ point

# LIST OF SYMBOLS

$a_i$	Actual measured value of a for $i^{th}$ point
$b_i$	Actual measured value of b for $i^{th}$ point
$A$	Matrix of actual a and b measured coordinates
$\hat{x}$	Least square estimate of slopes
$\delta$	A perturbation
D	Matrix relating perturbations in $\phi$ and $\xi$ with those in h, a and b
$G_a$	Stereo angles matrix relating perturbations in $\alpha, \beta, \theta$ and L with those in h, a and b
$G_r$	Stereo range matrix relating perturbations in M, N, K, L and J with those in h, a and b
$G_{ns}$	Non-stereo system matrix relating perturbations in R, $\beta, \theta$ and with those in h, a and b
Y	Covariance matrix of the variables
E	Expected value
$Y_a$	Covariance matrix of the variables for stereo angles
$Y_r$	Covariance matrix of the variables for stereo range
F	Matrix relating the slope estimate with the perturbations in h and A
dSg	Derivative of gradient
$\sigma_{sg}$	Standard deviation in gradient
$\sigma_\phi$	Standard deviation in roll angle $\phi$
$\sigma_\xi$	Standard deviation in pitch angle $\xi$
$\sigma_L$	Standard deviation in separation distance L
$\sigma_J$	Standard deviation in separation distance J
$\sigma_A$	Standard deviation in an angular measurement
$\sigma_\alpha$	Standard deviation in $\alpha$
$\sigma_\beta$	Standard deviation in $\beta$
$\sigma_\theta$	Standard deviation in $\theta$
$\sigma_R$	Standard deviation in a range measurement R
$\sigma_M$	Standard deviation in range measurement M
$\sigma_N$	Standard deviation in range measurement N
$\sigma_K$	Standard deviation in range measurement K



# LIST OF SYMBOLS

$c$	Data point spacing (meters)
$b^*$	Distance from vehicle (meters)
$\sigma_{h'}$	Standard deviation in $h'$ coordinate calculation
$\sigma_{a'}$	Standard deviation in $a'$ coordinate calculation
$\sigma_{b'}$	Standard deviation in $b'$ coordinate calculation
$\bar{\phantom{x}}$	Bar - denotes actual value (assumed errorless)

#### ACKNOWLEDGEMENT

The author would like to thank the National Aeronautics and Space Administration for sponsoring this research.

Dan Palumbo and Glen Herb provided very helpful information on laser rangefinders and scanning systems. Special thanks are extended to Paul Burger who developed much of the stochastic estimating method.

Most of all the author wishes to express his gratitude to Dr. C. N. Shen for his encouragement, helpful criticism and patient guidance during this project.

## ABSTRACT

The R.P.I. Martian Roving Vehicle requires an autonomous obstacle detection and path selection system. A laser rangefinder will be used to determine the locations of a number of discrete points at distances of 3 to 30 meters from the vehicle. The system might measure angles, ranges or a combination of both types of measurements.

The slope of the terrain is very important in the selection of a navigable path. Four, or more, terrain data points may be used to calculate a stochastic estimate of the gradient of a small area of the Martian surface in the vicinity of the points. The accuracy of this estimate is influenced by the point locations as well as the measurement errors.

The accuracy of stochastic gradient estimates is analyzed for two stereo-measurement systems, one measuring angles, and the other ranges. These are compared with a non-stereo system using a combination of measurements. The accuracy of the discrete point location calculations is also discussed.

The non-stereo system is shown to be the most compatible with present laser rangefinder technology.

## PART 1

### INTRODUCTION

The roundtrip communication time from Mars to Earth is over 40 minutes. Therefore, the R.P.I. Martian vehicle's terrain modeling and path selection system must be autonomous.

Two points along the path of the vehicle determine an in-path slope, while those across the path determine a cross-path slope. In the 3 to 30 meter range, however, inaccuracy in measurement can introduce very large errors in the computed slopes, which are the main factors in path selections. There are some threshold values for these slopes and heights above which a change of path is required. [1]

One system discussed in this report, referred to as stereo angles, uses three angular measurements in elevation and azimuth to locate a terrain point. Another system, called stereo range, uses three range measurements. These two systems are compared with a non-stereo system which uses one range, and two angular measurements in elevation and azimuth. [2]

A stochastic estimate of the gradient of the terrain may be computed using four or more terrain measurement points. The accuracy of this estimate depends on the terrain point locations and on the measurement errors. Since the R.P.I. vehicle will probably use a laser system to measure the terrain point coordinates, the accuracy requirements can be compared with the limits of present laser rangefinder technology. [3]

## PART 2

### METHOD OF APPROACH

The gradients or maximum slopes of the terrain in front of the vehicle are determined by measuring four or more points on the Martian surface.

#### A. Transformation of Coordinate Systems

##### 1. Stereo Angles

The elevation angles  $\alpha$  and  $\beta$ , and the azimuthal angle  $\theta$  are measured with respect to the coordinate system  $h'$ ,  $a'$ ,  $b'$  fixed to the vehicle as shown in Figure 1. A laser is located at point T which is 3 meters in height. The elevation angle  $\beta$  of the transmitted light beam is measured at T from the horizon to the terrain point U. The elevation angle  $\alpha$  of the received beam is measured at a point L meters from the top of the mast. Some type of scanning detector is assumed in the measurement of the angle  $\alpha$ . The angle  $\theta$  is the azimuthal angle of the transmitted beam.

From the geometry, with a sensor mast height of 3 meters, the terrain point coordinates  $h'$ ,  $a'$ ,  $b'$  are found in terms of  $\alpha$ ,  $\beta$ ,  $\theta$ , and L.

$$h' = 3 - \frac{L \tan \beta}{(\tan \beta - \tan \alpha)} \quad (1a)$$

$$a' = \frac{L \sin \theta}{(\tan \beta - \tan \alpha)} \quad (1b)$$

$$b' = \frac{L \cos \theta}{(\tan \beta - \tan \alpha)} \quad (1c)$$

The  $h'$ ,  $a'$ ,  $b'$  coordinate system which is fixed to the vehicle

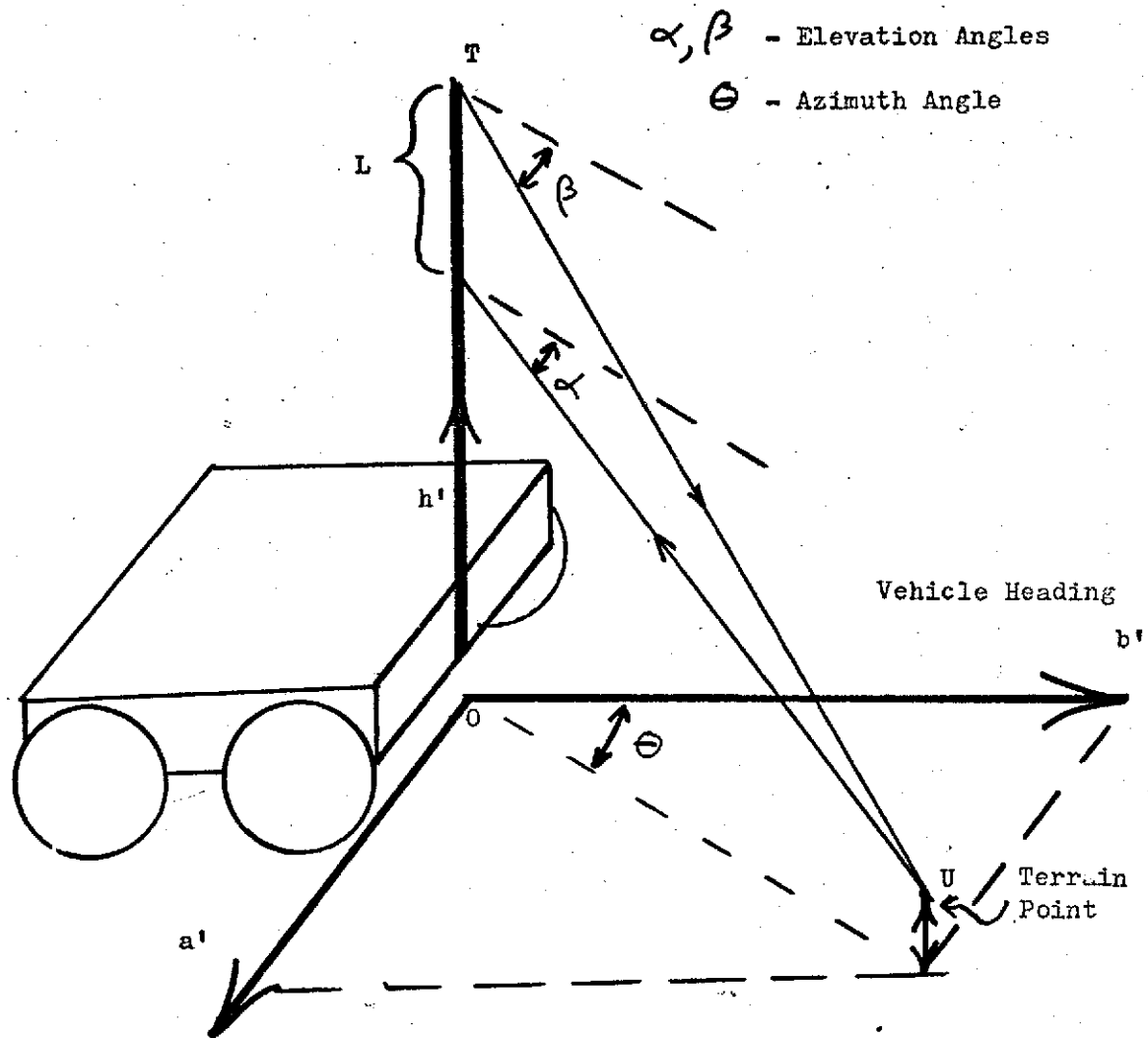


Figure 1 Stereo Angles System Coordinates

may be transformed to a reference system,  $h, a, b$  formed by the local vertical, the vehicle heading and an axis perpendicular to both. It is assumed that the vehicle rolls with an angle  $\phi$  and pitches with an angle  $\xi$  about the reference frame,  $h, a, b$ . In matrix form this transformation is: [4]

$$\begin{bmatrix} h \\ a \\ b \end{bmatrix} = C(\phi) B(\xi) \begin{bmatrix} h' \\ a' \\ b' \end{bmatrix} \quad (2a)$$

where

$$C(\phi) = \begin{bmatrix} \cos \phi & -\sin \phi & 0 \\ \sin \phi & \cos \phi & 0 \\ 0 & 0 & 1 \end{bmatrix} \quad (2b)$$

and

$$B(\xi) = \begin{bmatrix} \cos \xi & 0 & \sin \xi \\ 0 & 1 & 0 \\ -\sin \xi & 0 & \cos \xi \end{bmatrix} \quad (2c)$$

## 2. Stereo Range

The quantities  $M, N$  and  $K$  are measured with respect to the coordinate system  $h', a', b'$  which is fixed to the vehicle as in Fig. 2. The measurement  $M$  is twice the range to the terrain point  $U$  from the transmitter and receiver at  $T$  on top of the sensor mast.

$$M = 2 R \quad (3a)$$

The measurement  $N$  is the sum of the ranges from the transmitter at  $T$  to the terrain point  $U$  and from this point back to a receiver at a vertical distance  $L$  meters from the transmitter.

$$N = R + P \quad (3b)$$

The measurement  $K$  is the sum of the ranges from the transmitter at  $T$  to the terrain point  $U$  and from this point back to another receiver

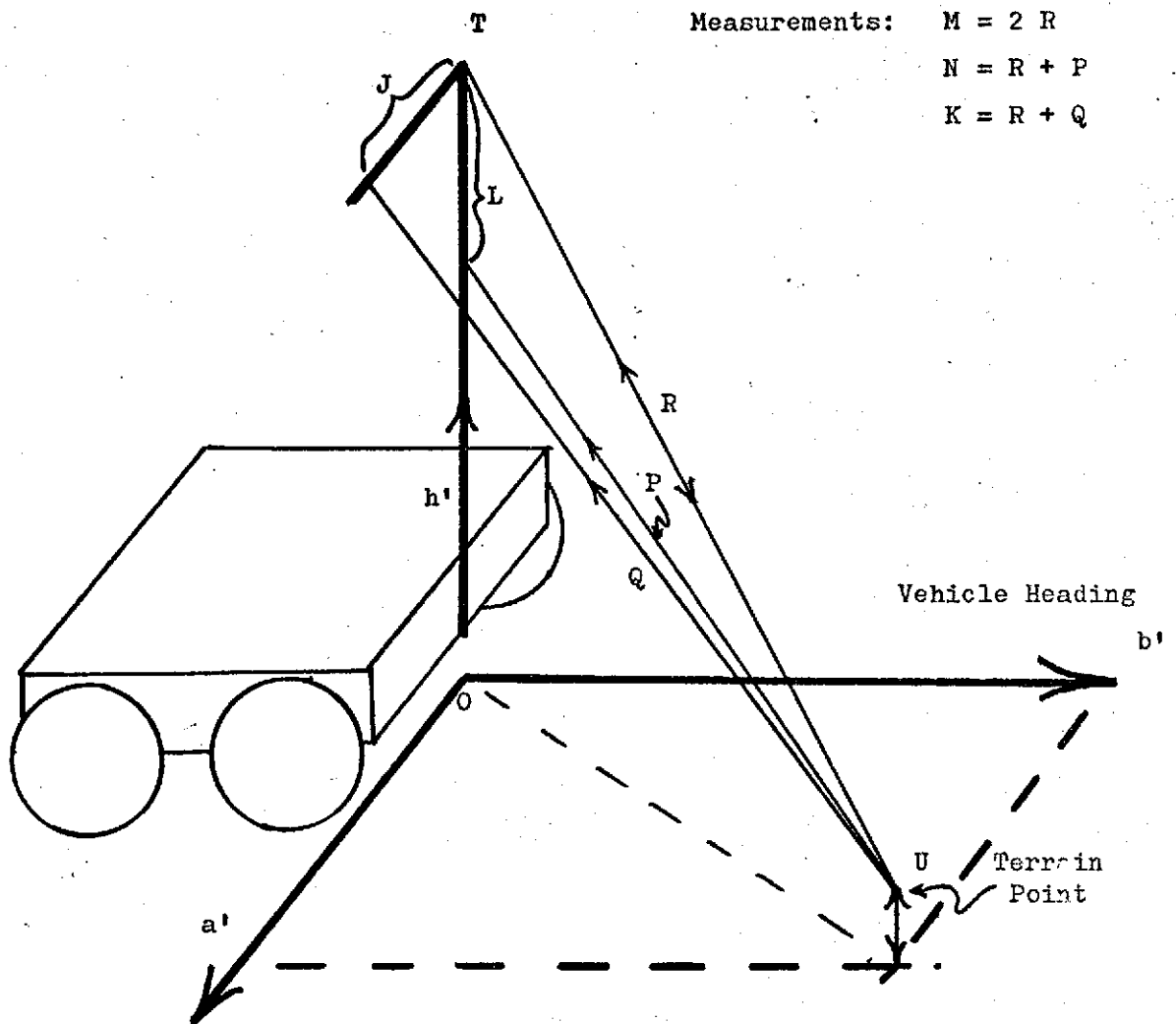


Figure 12 Stereo Range System Coordinates



at a horizontal distance J meters from the transmitter.

$$K = R + Q. \quad (3c)$$

From the geometry the coordinates of the terrain points are found in terms of M, N, K, L and J.

$$h' = 3 - \frac{L}{2} + \frac{N(N-M)}{2L} \quad (4a)$$

$$a' = \frac{K(M-K)}{2J} + \frac{J}{2} \quad (4b)$$

$$b' = \left[ \begin{aligned} &\frac{M^2}{4} - \frac{L^2}{4} - \frac{J^2}{4} + \frac{N(N-M)}{2} - \frac{K(M-K)}{2} \\ &- \frac{K^2(M-K)^2}{4J^2} - \frac{N^2(N-M)^2}{4L^2} \end{aligned} \right]^{\frac{1}{2}} \quad (4c)$$

The coordinate transformation from the  $h'$ ,  $a'$ ,  $b'$  system to the non-rotating system  $h$ ,  $a$ ,  $b$  has been shown in equation (2).

### 3. Non-stereo System [2]

The quantities  $R$ ,  $\beta$ , and  $\theta$  are measured with respect to the  $h'$ ,  $a'$ ,  $b'$  coordinate system as in Figure 3.

From the figure

$$h' = 3 - R \sin \beta \quad (5a)$$

$$a' = R \cos \beta \sin \theta \quad (5b)$$

$$b' = R \cos \beta \cos \theta \quad (5c)$$

Again the transformation to the non-rotating coordinate system is given by equation (2).

### B. Determinations of Slopes and Gradients

A number of the measurement points from a small area of the Martian surface, perhaps 1 meter by 1 meter, can be used to determine a plane in space. This may be written as

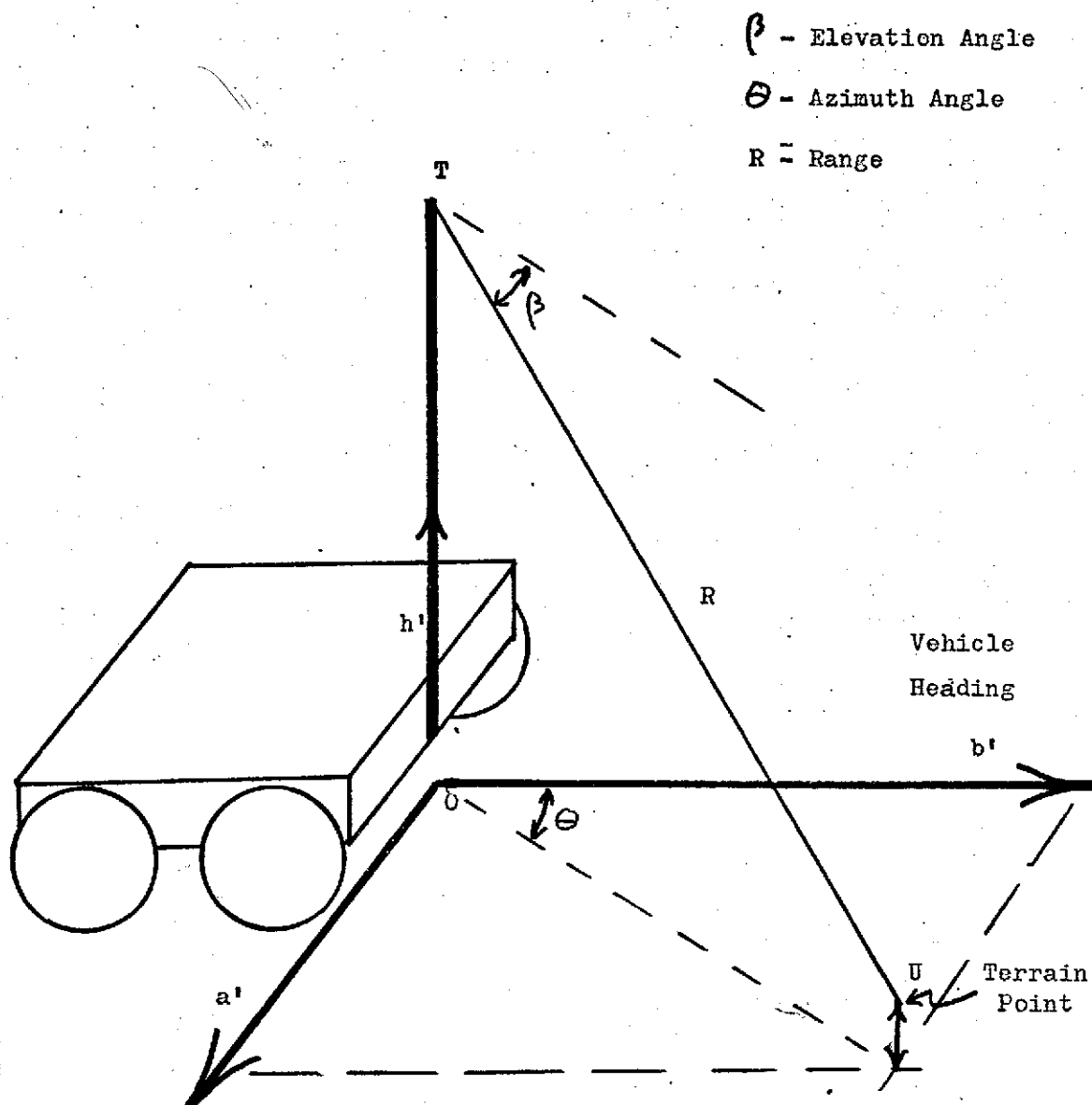


Figure 3 Non-stereo System Coordinates

$$h = ax_1 + bx_2 + x_3 \quad (6)$$

where the parameters  $x_1$  and  $x_2$  are constants. Equation (6) is differentiated to give

$$\partial h = \frac{\partial h}{\partial a} da + \frac{\partial h}{\partial b} db = x_1 da + x_2 db$$

where

$$x_1 = \frac{\partial h}{\partial a} = \text{cross-path slope}$$

$$x_2 = \frac{\partial h}{\partial b} = \text{in-path slope} \quad [5,6]$$

The gradient of the plane is defined as

$$Sg = (x_1^2 + x_2^2)^{\frac{1}{2}} \quad (7)$$

The gradient is the maximum slope of the terrain plane representing the local terrain feature. If the magnitude of the gradient is less than some critical value, probably about 25 degrees, the terrain will be considered passable.

By using the measurement points to locate a plane, Equation (6) may be written as

$$h_i = a_i x_1 + b_i x_2 + x_3 \quad (8)$$

where  $h_i$ ,  $a_i$  and  $b_i$  can be found either from  $\alpha, \beta, \theta$  and  $L$  for a stereo angles system using Equations (1) and (2), from  $M, N, K, L$  and  $J$  for a stereo range system using Equations (4) and (2) or from  $R, \beta$  and  $\theta$  for the non-stereo system using Equations (5) and (2).

Three points theoretically determine a plane. To obtain greater accuracy, however, four or even six points can be used to determine the gradient. A number of adjacent planes, each covering a small area, may be modeled to construct a complete picture of the terrain in front

of the vehicle.

### PART 3

#### ESTIMATION OF SLOPES AND THEIR COVARIANCES

This section includes the solutions of a least squares error estimate and the covariance matrices when  $n > 3$ .

##### A. Least Square Estimate of the Slopes

A least square error estimate can be performed minimizing

$$\sum_{i=1}^n (\hat{h}_i - \bar{h}_i)^2 \quad (9)$$

assuming  $a_i = \bar{a}_i$  and  $b_i = \bar{b}_i$  are true in Equation (8). The value  $\bar{h}_i$  is the actual measured height of the terrain point and  $\hat{h}_i$  is the corresponding height in the modeled plane.

Equation (8) is written in matrix form as

$$\bar{h} = \bar{A} x \quad (10)$$

or

$$\begin{bmatrix} \bar{h}_1 \\ \bar{h}_2 \\ \vdots \\ \bar{h}_n \end{bmatrix} = \begin{bmatrix} \bar{a}_1 & \bar{b}_1 & 1 \\ \bar{a}_2 & \bar{b}_2 & 1 \\ \vdots & \vdots & \vdots \\ \bar{a}_n & \bar{b}_n & 1 \end{bmatrix} \begin{bmatrix} x_1 \\ x_2 \\ x_3 \end{bmatrix} \quad n=4 \text{ or } 6$$

The matrix  $x$  must be determined in such a way that Equation (9) is minimized. Through use of the Gram-Schmidt orthogonalization procedure the least square estimate of  $x$  becomes [7]

$$\hat{x} = (\bar{A}^T \bar{A})^{-1} \bar{A}^T \bar{h} \quad (11)$$

##### B. Perturbation of the Variables

The matrix  $A$  in the least square estimate above is assumed to be completely deterministic. [8] The determination of  $h$ ,  $a$ , and  $b$  involves errors due to uncertainties in the measured angles or ranges.

The symbol  $\delta$  is used to denote a perturbation.

### 1. Stereo Angles

Then  $\delta h$ ,  $\delta a$  and  $\delta b$  can be found in terms of  $\delta\phi$ ,  $\delta\zeta$ ,  $\delta\beta$ ,  $\delta\alpha$ ,  $\delta\theta$  and  $\delta L$ . From Equations (1) and (2) the perturbations in  $h$ ,  $a$  and  $b$  are determined as follows:<sup>2</sup>

$$\begin{bmatrix} \delta h \\ \delta a \\ \delta b \end{bmatrix} = D(h^i, a^i, b^i, \phi, \zeta) \begin{bmatrix} \delta\phi \\ \delta\zeta \end{bmatrix} + C(\phi) B(\zeta) G_a(\alpha, \beta, \theta, L) \begin{bmatrix} \delta\alpha \\ \delta\beta \\ \delta\theta \\ \delta L \end{bmatrix} \quad (12a)$$

where

$$G_a(\alpha, \beta, \theta, L) = \begin{bmatrix} \frac{L \tan\theta \sec^2\alpha}{(\tan\beta - \tan\alpha)^2} & \frac{L \tan\theta \sec^2\beta}{(\tan\beta - \tan\alpha)^2} & 0 & \frac{\tan\theta}{(\tan\beta - \tan\alpha)} \\ \frac{L \sec^2\alpha \sin\theta}{(\tan\beta - \tan\alpha)^2} & \frac{L \sec^2\beta \sin\theta}{(\tan\beta - \tan\alpha)^2} & \frac{L \cos\theta}{(\tan\beta - \tan\alpha)} & \frac{\sin\theta}{(\tan\beta - \tan\alpha)} \\ \frac{L \sec^2\alpha \cos\theta}{(\tan\beta - \tan\alpha)^2} & \frac{L \sec^2\beta \cos\theta}{(\tan\beta - \tan\alpha)^2} & \frac{-L \sin\theta}{(\tan\beta - \tan\alpha)} & \frac{\cos\theta}{(\tan\beta - \tan\alpha)} \end{bmatrix} \quad (12b)$$

The derivation of the matrix  $D$  is shown in Appendix A.

### 2. Stereo Range

The quantities  $\delta h$ ,  $\delta a$ , and  $\delta b$  can be found in terms of  $\delta\phi$ ,  $\delta\zeta$ ,  $\delta M$ ,  $\delta N$ ,  $\delta K$ ,  $\delta L$  and  $\delta J$ . From Equations (2) and (4) the perturbations in  $h$ ,  $a$  and  $b$  are determined as follows:

$$\begin{bmatrix} \delta h \\ \delta a \\ \delta b \end{bmatrix} = D(h^i, a^i, b^i, \phi, \zeta) \begin{bmatrix} \delta\phi \\ \delta\zeta \end{bmatrix} + C(\phi) B(\zeta) G_r(M, N, K, L, J) \begin{bmatrix} \delta M \\ \delta N \\ \delta K \\ \delta L \\ \delta J \end{bmatrix} \quad (13a)$$

where

$$G_r(M, N, K, L, J) = \begin{bmatrix} \frac{-N}{2L} & \frac{2N-M}{2L} & 0 & -\frac{1}{2} - \frac{N(N-M)}{2L^2} & 0 \\ \frac{K}{2J} & 0 & \frac{M-2K}{2J} & 0 & \frac{1}{2} - \frac{K(M-K)}{2J^2} \\ \epsilon_{31} & \epsilon_{32} & \epsilon_{33} & \epsilon_{34} & \epsilon_{35} \end{bmatrix}$$

and

$$\begin{aligned} \epsilon_{31} &= \left[ \frac{\frac{M}{2} - \frac{N}{2} - \frac{K}{2} - \frac{K^2(M-K)}{2J^2} + \frac{N^2(N-M)}{2L^2}}{2b^1} \right] \\ \epsilon_{32} &= \left[ \frac{\frac{2N-M}{2} - \frac{(2N^3 - 3N^2M + NM^2)}{2L^2}}{2b^1} \right] \\ \epsilon_{33} &= \left[ \frac{\frac{2K-M}{2} - \frac{(2K^3 - 3K^2M + KM^2)}{2J^2}}{2b^1} \right] \\ \epsilon_{34} &= \left[ \frac{\frac{N^2(N-M)^2}{2L^3} - \frac{L}{2}}{2b^1} \right] \\ \epsilon_{35} &= \left[ \frac{\frac{K^2(M-K)^2}{2J^3} - \frac{J}{2}}{2b^1} \right] \end{aligned} \quad (13b)$$

For the non-stereo system the matrix G becomes [2]

$$G_{ns}(R, \beta, \Theta) = \begin{bmatrix} (-\sin \beta) & (-R \cos \beta) & 0 \\ (\cos \beta \sin \Theta) & (-R \sin \beta \sin \Theta) & (R \cos \beta \cos \Theta) \\ (\cos \beta \cos \Theta) & (-R \sin \beta \cos \Theta) & (-R \cos \beta \sin \Theta) \end{bmatrix} \quad (14)$$

### C. The Covariance Matrix of the Variables

The covariance matrix of the variables may be defined as [9]

$$Y = E \left\{ \begin{bmatrix} \delta_h \\ \delta_a \\ \delta_b \end{bmatrix} \begin{bmatrix} \delta_h & \delta_a & \delta_b \end{bmatrix} \right\}$$

The symbol E denotes expected value.

#### 1. Stereo Angles System

If  $\delta\phi, \delta\xi, \delta\alpha, \delta\beta, \delta\theta$  and  $\delta L$  are not correlated, [9] then from Appendix B the following relation is obtained.

$$Y_a = D \begin{bmatrix} E(\delta\phi)^2 & 0 \\ 0 & E(\delta\xi)^2 \end{bmatrix} D^T + C B G_a \begin{bmatrix} E(\delta\alpha)^2 & 0 & 0 & 0 \\ 0 & E(\delta\beta)^2 & 0 & 0 \\ 0 & 0 & E(\delta\theta)^2 & 0 \\ 0 & 0 & 0 & E(\delta L)^2 \end{bmatrix} G_a^T B^T C^T \quad (16)$$

The variances of h, a and b are the diagonal elements of the matrix Y in Equation (15). The standard deviation of each of these quantities is the square root of its variance. From Equations (15) and (16) the standard deviations of h, a and b can be computed in terms of those of  $\phi, \xi, \alpha, \beta, \theta$  and L for each point. These are known quantities which depend on the accuracy of the measuring devices.

#### 2. Stereo Range System

If  $\delta\phi, \delta\xi, \delta M, \delta N, \delta K, \delta L$  and  $\delta J$  are uncorrelated [9] then by the same method used to derive Equation (16) the following is obtained.

$$Y_r = D \begin{bmatrix} E(\delta\phi)^2 & 0 \\ 0 & E(\delta\zeta)^2 \end{bmatrix} D^T + C B G_r \begin{bmatrix} E(\delta M)^2 & 0 & 0 & 0 & 0 \\ 0 & E(\delta N)^2 & 0 & 0 & 0 \\ 0 & 0 & E(\delta K)^2 & 0 & 0 \\ 0 & 0 & 0 & E(\delta L)^2 & 0 \\ 0 & 0 & 0 & 0 & E(\delta J)^2 \end{bmatrix} G_r^T B^T C^T \quad (17)$$

The standard deviations of  $h$ ,  $a$  and  $b$  can be computed in terms of those of  $\phi$ ,  $\zeta$ ,  $M$ ,  $N$ ,  $K$ ,  $L$ , and  $J$  for each point. Equations (16) and (17) include the matrix  $G$  which involves all the measured quantities. Therefore, the standard deviations in  $h$ ,  $a$  and  $b$  depend on the locations of the data points in relation to the vehicle as well as on the accuracies of these measurements.

#### D. Covariance Matrix of the Slopes

Equation (10) may be rewritten to include the perturbations in  $h$ ,  $A$  and  $x$ .

$$h = A x \quad (18a)$$

$$h = \bar{h} + \delta h \quad (18b)$$

$$A = \bar{A} + \delta A \quad (18c)$$

$$x = \bar{x} + \delta x \quad (18d)$$

The original equation, (10), is subtracted from (16a) to obtain

$$\delta h \approx \bar{A} \delta x + \delta A \bar{x} \quad (19)$$

The estimate of the slope is

$$\hat{\delta x} = F(\delta h - \delta A \bar{x}) \quad (20)$$



Equations (19) and (20) are compared to Eq.(10) leading to the result that

$$F = (\bar{A}^T \bar{A})^{-1} \bar{A}^T \quad (21)$$

The covariance matrix of the slopes is determined in Appendix C as

$$E(\hat{\delta x} \hat{\delta x}^T) = F \{ E(\delta h \delta h^T) - E(\delta A \bar{x} \delta h^T) - E(\delta h (\delta A \bar{x})^T) + E(\delta A \bar{x} (\delta A \bar{x})^T) \} F^T \quad (22)$$

where

$$\hat{\delta x} = \begin{bmatrix} \hat{\delta x}_1 \\ \hat{\delta x}_2 \\ \vdots \\ \hat{\delta x}_n \end{bmatrix} \quad \delta h = \begin{bmatrix} \delta h_1 \\ \delta h_2 \\ \vdots \\ \delta h_n \end{bmatrix} \quad \delta A \bar{x} = \begin{bmatrix} (\delta a_1 \bar{x}_1 + \delta b_1 \bar{x}_2) \\ (\delta a_2 \bar{x}_1 + \delta b_2 \bar{x}_2) \\ \vdots \\ (\delta a_n \bar{x}_1 + \delta b_n \bar{x}_2) \end{bmatrix} \quad (23)$$

The matrix A is in terms of a and b, Therefore,  $\delta h$  and  $\delta A$  can be expressed as functions of  $\delta \phi, \delta \zeta, \delta \alpha, \delta \theta$  and  $\delta L$  for the stereo angles system, using Eq. (12). Thus Eq. (22) can be evaluated as shown in Appendix C.

For the stereo range system  $\delta h$  and  $\delta A$  are expressed as functions of  $\delta \phi, \delta \zeta, \delta M, \delta K, \delta N, \delta L$  and  $\delta J$  using Equation (13). Then the covariance matrix of the slopes is determined in Equation (22).

From Equations (21) and (22) it is seen that the covariance matrix of the slopes also depends on the matrix  $\bar{A}$  which is determined by the measured locations of the points. As a result the estimate of the gradient is expected to be influenced by the data point spacing.

#### E. Variance of the Gradient

The symbol  $\sigma_{sg}$  denotes the standard deviation of the gradient Sg. Equation (7) is differentiated to get

$$dSg = (x_1^2 + x_2^2)^{-\frac{1}{2}} x_1 dx_1 + (x_1^2 + x_2^2)^{-\frac{1}{2}} x_2 dx_2 \quad (24)$$

From Equation (24) the variance of the gradient becomes [10]

$$\sigma_{sg}^2 = \frac{\bar{x}_1^2}{(\bar{x}_1^2 + \bar{x}_2^2)} \sigma_{x_1}^2 + 2 \frac{\bar{x}_1 \bar{x}_2}{(\bar{x}_1^2 + \bar{x}_2^2)} \sigma_{x_1 x_2}^2 + \frac{\bar{x}_2^2}{(\bar{x}_1^2 + \bar{x}_2^2)} \sigma_{x_2}^2 \quad (25)$$

where

$$\begin{aligned} \sigma_{x_1}^2 &= E[(\hat{\delta}_{x_1})^2] \\ \sigma_{x_2}^2 &= E[(\hat{\delta}_{x_2})^2] \\ \sigma_{x_1 x_2}^2 &= E[(\hat{\delta}_{x_1} \hat{\delta}_{x_2})] \end{aligned}$$

These covariances are found from Equation (22).

The value of  $\sigma_{sg}$  is an estimate of the accuracy of the estimation of the gradient. If a normal distribution is assumed, then the true value of the random variable, in this case the gradient, will lie within one standard deviation of the estimated value 68% of the time.<sup>[9]</sup> The actual gradient will be within two standard deviations of the estimate 95% of the time.

For example, if the estimate of gradient is  $25^\circ$  and  $\sigma_{sg} = 3^\circ$  then it is only a 68% probability that the actual gradient of the terrain is between  $22^\circ$  and  $28^\circ$ . If the estimated gradient is near the maximum passable value, the magnitude of  $\sigma_{sg}$  is very important in the operation of the path selection algorithm.

The slope covariances depend on the data point locations in relation to the vehicle and to each other. The standard deviation of gradient  $\sigma_{sg}$  depends on the slope covariances, so  $\sigma_{sg}$  will also be a function of the data point locations. Varying the spacing of these points changes the covariance matrix and therefore affects  $\sigma_{sg}$ .

#### F. Determination of the Gradient

Once the value of the cross-path and in-path slopes are determined from the least squares estimate, the gradient can be calculated from Eq. (7). The vehicle uses the estimate of gradient in its path selection algorithm<sup>[1]</sup> to select a safe course.

### PART 4

#### DISCUSSION OF NUMERICAL RESULTS

It is assumed that the vehicle will have some type of scanning apparatus to let the laser beam arrive at various terrain points.<sup>[11]</sup> The  $h'$ ,  $a'$  and  $b'$  coordinates will be computed either by stereo angles or stereo ranges and then transformed to the non-rotating coordinate system  $h$ ,  $a$  and  $b$  as described in section 2A.

Four or more data points are used to model a plane and to calculate a least squares estimate of the gradient as outlined in Part 3. The accuracy of this estimate depends on the magnitudes of the cross-path and in-path slopes, the distance of the data points from the vehicle, the spacing between the points and the roll and pitch angles.

It is assumed that the measurements  $\phi$  and  $\zeta$  will provide standard deviations  $\sigma_\phi$  and  $\sigma_\zeta$  of about  $1^\circ$ .<sup>[2]</sup> By assuming reasonable data point spacing, previous research<sup>[2]</sup> has shown that  $\sigma_{sg}$  is approximately  $30^\circ$  if  $\sigma_\phi = \sigma_\zeta = 1^\circ$ . This value for the standard deviation in gradient is unacceptable. It is desired that  $\sigma_{sg}$  be less than  $2^\circ$  or  $3^\circ$  for terrain within the 3 to 30 meter range.

If a rapid-scan laser is used, the effect of  $\sigma_\phi$  and  $\sigma_\zeta$  can be reduced. If the time between the measurement of adjacent data points

is on the order of milli-seconds, as it would be with a rapid-scan laser, then the data points are measured almost instantaneously compared to the vehicle motion which is on the order of seconds. All four points will then have the same values of  $\phi$  and  $\xi$ . The points will retain their relative position when they are transformed to the non-rotating coordinate system by Eq. (2). Therefore, the planes can be modeled in the  $h', a', b'$  coordinate system and then transformed to the  $h, a, b$  coordinate system. By letting  $\phi = \xi = 0^\circ$  in Equations (12) and (16), or (13) and (17), then the result is that  $h' = h$ ,  $a' = a$ , and  $b' = b$  in those equations. The additive effect of the standard deviation in  $\phi$  and  $\xi$  will be about  $1^\circ$  because with the rapid-scan laser the effects of  $\sigma_\phi$  and  $\sigma_\xi$  can be added to the factor  $\sigma_{sg}$  from the modeled plane afterward since the entire plane is transferred at the same time to the non-rotating coordinate system. As a result, in the calculation of  $\sigma_{sg}$  the substitution  $\sigma_\phi = \sigma_\xi = 0^\circ$  is made in Equations (16) and (17).

The maximum magnitude of navigable slope is assumed to be  $25^\circ$ . Relative slopes between  $+50^\circ$  and  $-50^\circ$  are possibly navigable as shown in Figure 4. The following analysis considers relative slopes within these limits.

#### 1. Stereo Angles System

It is assumed that the scanning mechanism can provide any desired data point spacing at distances from 3 to 30 meters from the vehicle. The data point spacing also depends on terrain irregularities, however, a flat terrain is assumed at the start.

The distance  $L$  in Fig. 1 is assumed to be 1.0 meter. This is the most reasonable value for a 3 meter sensor mast height. A larger value of  $L$  can give smaller errors in measurement. But, as  $L$  is

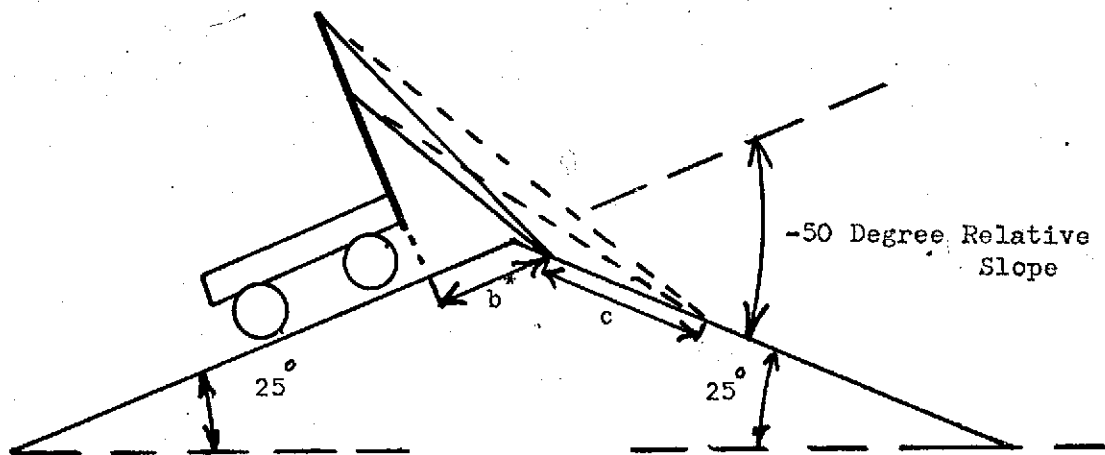
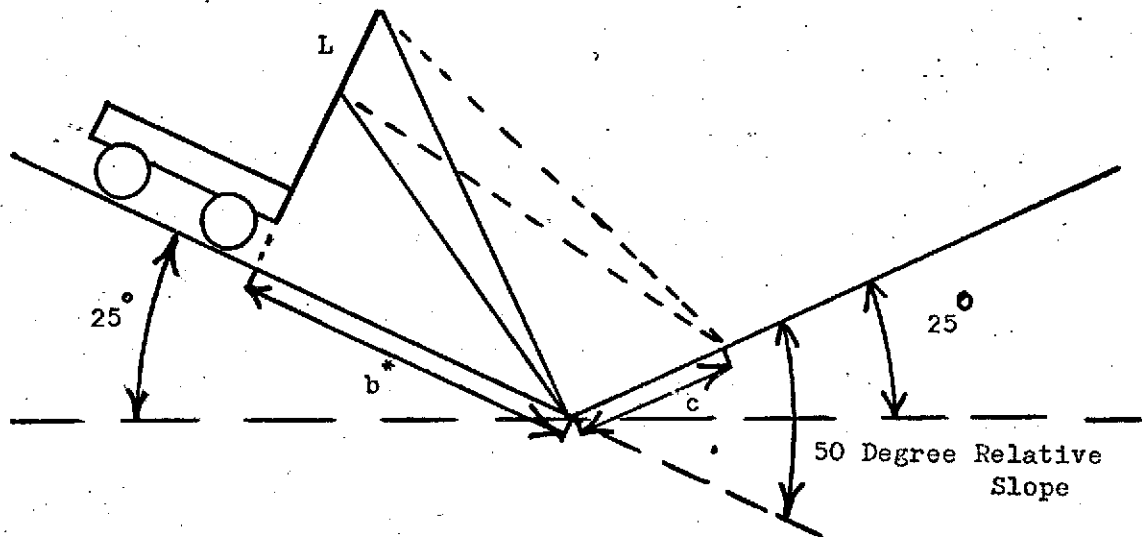


Figure 4 Relative In-Path Slopes

increased beyond one meter, the vehicle's ability to observe negative slopes is decreased. Also, if the receiver is lower on the mast there is more chance that the reflected laser beam will be blocked by other vehicle equipment. 1

The standard deviations  $\sigma_\alpha$ ,  $\sigma_\rho$  and  $\sigma_\theta$  are set equal to 1', a reasonable value using presently available equipment. [3] Then the data point spacing and the standard deviation  $\sigma_L$  are varied for points in the 3 to 30 meter range. In order to determine  $\sigma_{sg}$ , the standard deviations of the measured values and the data point coordinates are obtained from Eqs. (12), (16), (21), (23) and (25).

Figure 5 shows a plot of standard deviation in gradient  $\sigma_{sg}$  vs. distance,  $b^*$ , from the vehicle for flat terrain with 0° relative slope having  $\sigma_L = 0.01m$ . The dotted lines are for  $\sigma_L = 0.005m$ . Clearly  $\sigma_L$  has an important effect on  $\sigma_{sg}$  for the stereo angles system, especially at close range where decreasing  $\sigma_L$  from 0.01m to 0.005m reduces the value of  $\sigma_{sg}$  by fifty percent. As expected, larger data point spacing gives smaller values for the standard deviation in gradient. At close range, data point spacing of 0.66m or less is required because 0.66 meters is the width of the widest navigable crevice. [1] At 4 meters distance from the vehicle, a spacing of 0.6m gives  $\sigma_{sg} = 3^\circ$  and  $1.55^\circ$  with  $\sigma_L = 0.01m$  and  $0.005m$  respectively. Since  $\sigma_{sg}$  is designed to be less than  $2^\circ$ , it appears that  $\sigma_L$  must be about 0.005 meter or less.

The standard deviation in the distance  $L$  ( $\sigma_L$ ) may result from changes in the sensor mast, expansion or contraction due to temperature changes, or from uncertainties caused by the laser

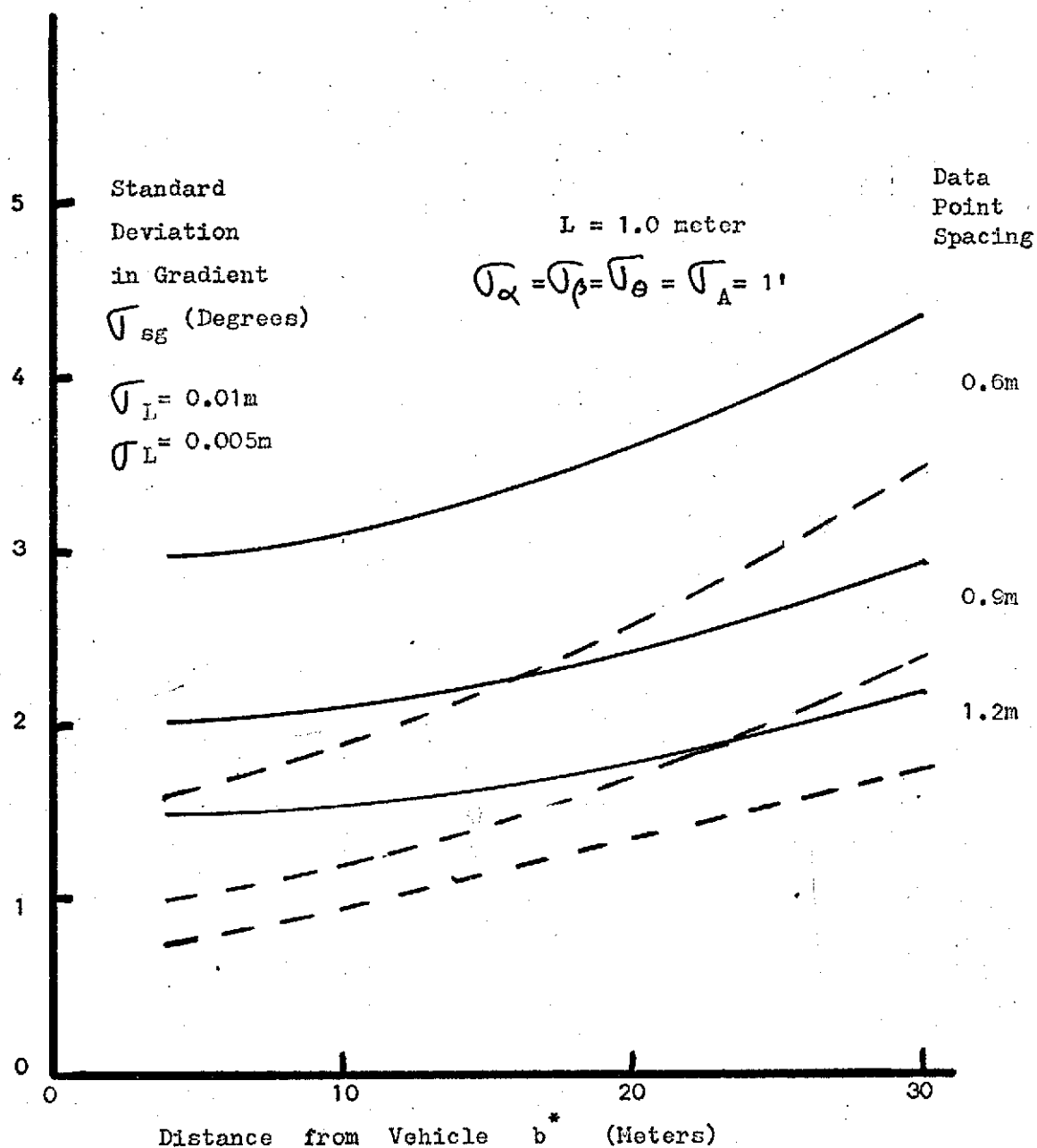


Figure 5 Stereo Angles System: Standard Deviation in Gradient Versus Distance from Vehicle on Flat Terrain with Relative Slope =  $0^\circ$

transmitter and receiver.

At ranges of 20 to 30 meters, a data point spacing of 1.2 m will be adequate to obtain the gradient of the terrain in front of the vehicle. This terrain would probably be remeasured when the vehicle moves closer to it. In Fig. 4, at 30 meters with 1.2 meter data point spacing, the computed results are that the standard deviations for gradient  $\sigma_{sg}$  are  $2.2^\circ$  and  $1.8^\circ$  for  $\sigma_L = 0.01m$  and  $\sigma_L = 0.005m$  respectively. At that range both values of the quantity  $\sigma_{sg}$  may be acceptable.

Figure 6 shows the plot of  $\sigma_{sg}$  versus relative in-path slope from  $-27^\circ$  to  $+50^\circ$  at a distance of 4 meters from the vehicle. The vehicle cannot measure negative in-path slopes of more than  $-27^\circ$  because the terrain obstructs the line of sight. The cross-path slope,  $\bar{x}_1$ , is set to  $0^\circ$  in Equations (19), (20), (22) and (25). The in-path slope,  $\bar{x}_2$ , varies from  $-27^\circ$  to  $+50^\circ$ . The standard deviations  $\sigma_L$  and  $\sigma_A$  are varied in Eq.(16) and the results used in Eqs. (22) and (25) to calculate the quantity  $\sigma_{sg}$ . In Fig. 6 the data point spacing is 0.6 meter as required at the 4 meter distance. The stereo angles system estimate of the standard deviation in gradient  $\sigma_{sg}$  is quite sensitive to the relative in-path slope.

By reducing the angular standard deviation,  $\sigma_A = \sigma_\alpha = \sigma_\beta = \sigma_\theta$ , to 6 arc-seconds and maintaining the transmitter-receiver separation distance standard deviation  $\sigma_L$  at 0.01m, the standard deviation in gradient  $\sigma_{sg}$  is not significantly reduced. If the quantity  $\sigma_L$  is set equal to zero and the quantity  $\sigma_A$  is set equal to 1' then  $\sigma_{sg}$  has a maximum value of  $2.5^\circ$  for relative in-path slope of  $+50^\circ$ . Increasing the magnitude of  $\sigma_L$  to 0.001m has a small effect on the value of  $\sigma_{sg}$ .



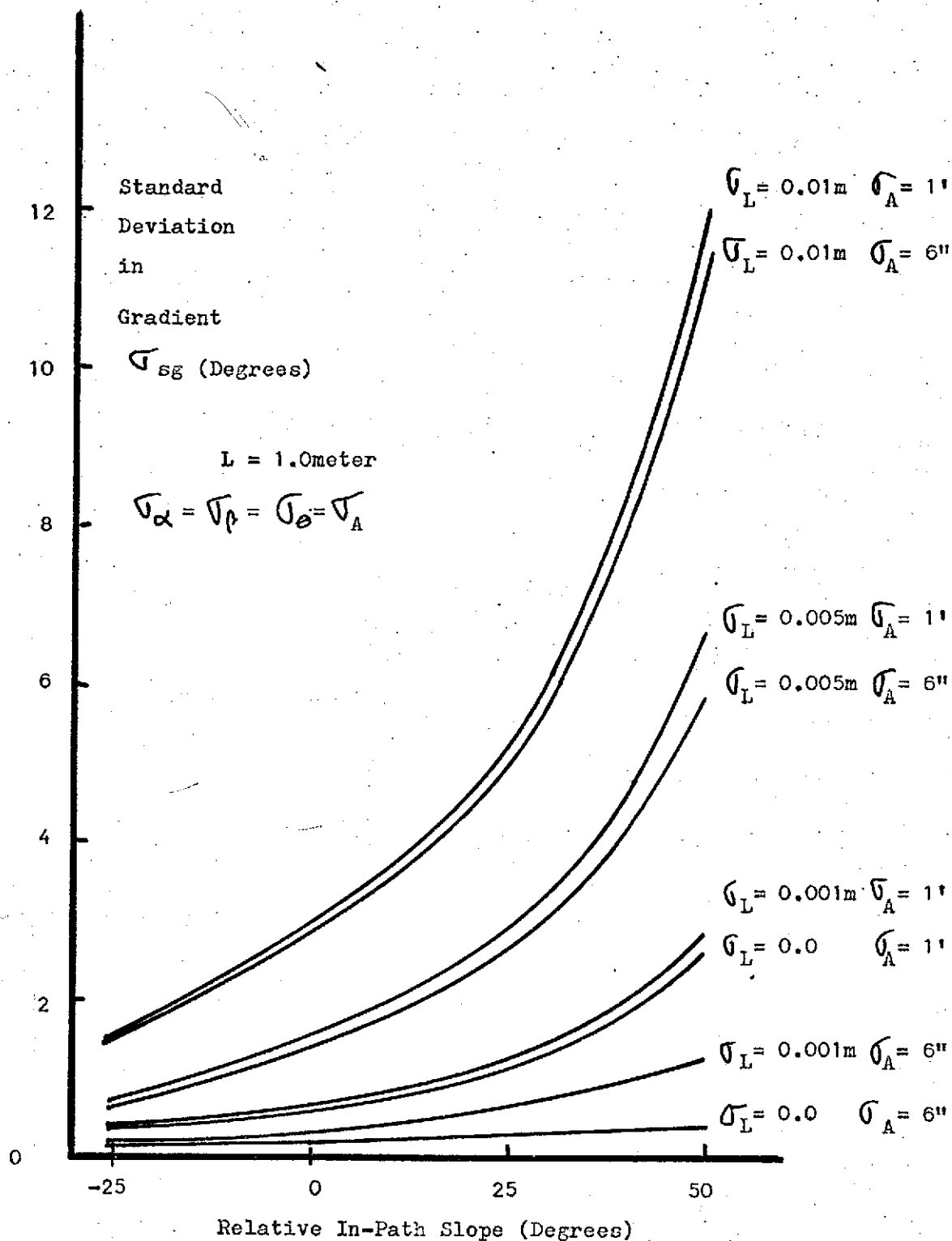


Figure 6 Stereo Angles System: Standard Deviation in Gradient Versus Relative In-Path Slopes for Terrain at 4m with Data Point Spacing=0.6m

Reducing the angular standard deviation to less than  $1'$  will require additional and more bulky equipment. Accuracy as low as 6 arc-seconds may not be practical but would improve the resulting  $\sigma_{sg}$  if  $\sigma_L$  is about 0.001 meter.

Figure 7 shows the standard deviation in gradient  $\sigma_{sg}$  vs. relative in-path slope from  $-6^\circ$  to  $+50^\circ$  at a distance of 20 meters from the vehicle. The terrain obstructs the view of the in-path slopes for more than  $-6^\circ$  relative slopes at 20 meters. For this graph the data point spacing is 1.2 meters. At 20 meters the standard deviation  $\sigma_{sg}$  increases drastically with increasing relative in-path slope. To obtain the quantity  $\sigma_{sg}$  less than  $3^\circ$  for all relative in-path slopes up to  $50^\circ$ , the standard deviations  $\sigma_L$  should be less than 0.001m and  $\sigma_A$  less than  $6''$ . Larger values of either standard deviation have the results of  $\sigma_{sg}$  being much greater than  $3^\circ$  for nearly all positive relative in-path slopes.

Figure 8 shows the standard deviation in gradient vs. relative cross-path slopes from  $0^\circ$  to  $+50^\circ$  for distances of 4 and 20 meters with data point spacings of 0.6 meters and 1.2 meters respectively. Cross-path slopes from  $0^\circ$  to  $-50^\circ$  will give the same results because of the symmetry of the system. If the standard deviations  $\sigma_A = 1'$  and  $\sigma_L = 0.005m$ , or less, the value of  $\sigma_{sg}$  is less than  $2.5^\circ$  at both distances.

## 2. Stereo Range System

As in the stereo angles system, it is assumed that the rapid scan transmitter at T (Fig.2) can provide the desired data point spacing for flat terrain. The separation distances L and J are both assumed to be equal to one meter. This is the most reasonable value

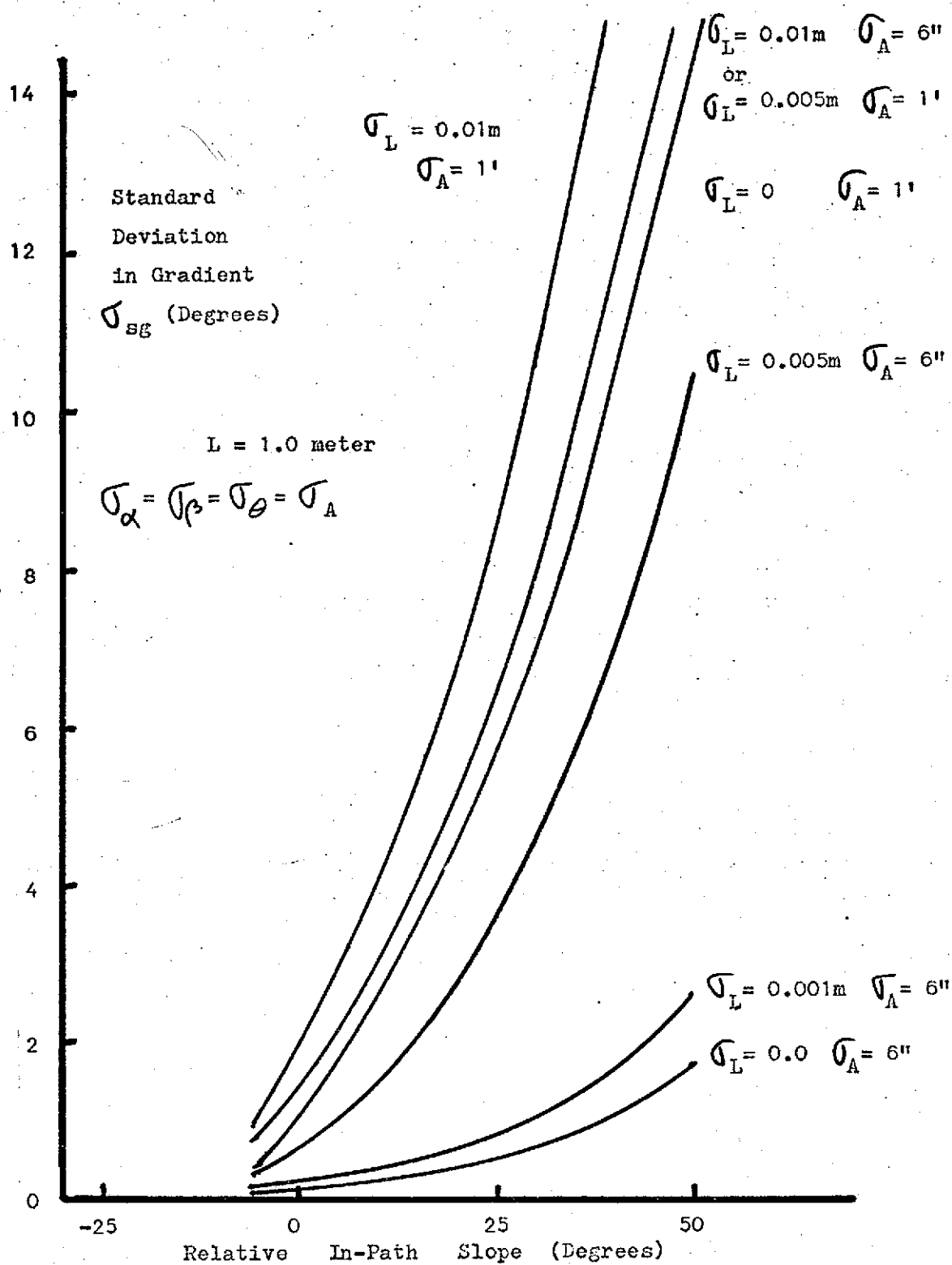


Figure 7 Stereo Angles System: Standard Deviation in Gradient Versus Relative In-Path Slope for Terrain at 20 Meters with Data Point Spacing 1.2m

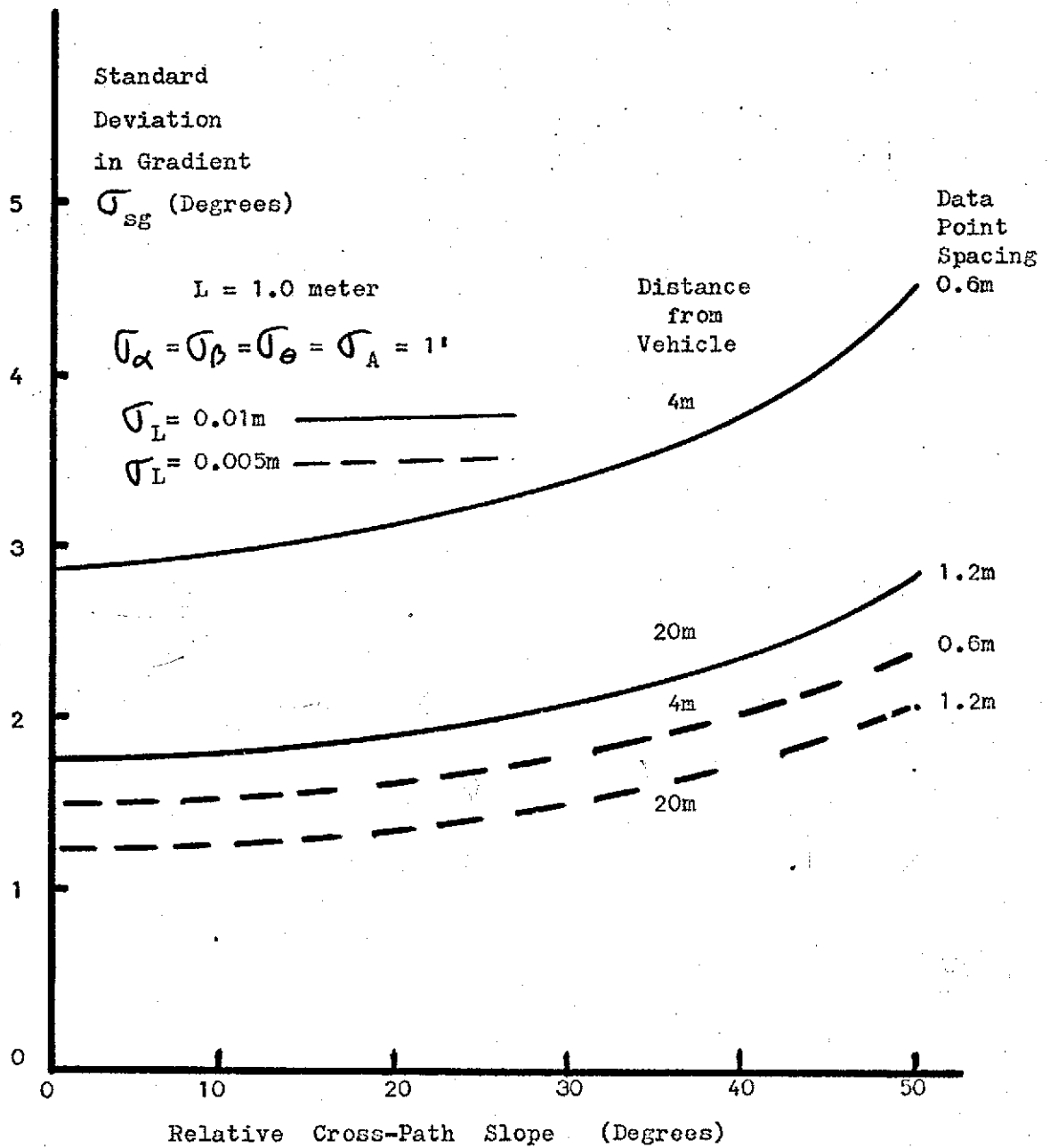


Figure 8 Stereoc Angles System: Standard Deviation in Gradient Versus Relative Cross-Path Slope for Terrain at 4 and 20 Meters

for the vertical separation distance  $L$  for the reasons stated previously. The one meter value is also reasonable for the horizontal separation distance  $J$  because a larger  $J$  will require a more massive support.

It is assumed that the standard deviations in  $L$  and  $J$  are equal since the system configuration is somewhat symmetric in the horizontal and vertical directions. These uncertainties may result from changes in the support dimensions and from the laser transmitter and its 3 receivers. [2,11]

The range standard deviations  $\sigma_M$ ,  $\sigma_N$ , and  $\sigma_K$  are all assumed equal to  $2\sigma_R$ . These standard deviations and the data point coordinates are employed to calculate the quantity  $\sigma_{sg}$  in Equations (13), (17), (21) and (25).

Figure 9 shows  $\sigma_{sg}$  vs. distance,  $b^*$ , from the vehicle for flat terrain with relative slopes =  $0^\circ$ , and  $\sigma_R = 0.001m$ . The solid lines show the quantity  $\sigma_{sg}$  when the value of  $\sigma_L = \sigma_J$  is  $0.01m$  and the dotted lines when  $\sigma_L = \sigma_J$  is  $0.005m$ . The standard deviations in gradient  $\sigma_{sg}$  for the stereo range system are not sensitive to the standard deviations in separation distances  $\sigma_L$  and  $\sigma_J$ . By reducing the quantity  $\sigma_L$  from  $0.01m$  to  $0.005m$  at a distance of 4 meters with point spacing of  $0.6m$  and range standard deviation  $\sigma_R = 0.001m$ , the value of  $\sigma_{sg}$  decreases from  $2.3^\circ$  down to  $1.7^\circ$ .

As expected, larger data point spacing results in smaller standard deviation in gradient. At close range a  $0.6m$  point spacing results in the quantity  $\sigma_{sg} = 2.3^\circ$  when the values of  $\sigma_R$  and  $\sigma_L$  are  $0.001m$  and  $0.01m$  respectively. To obtain standard deviation in gradient less than  $2^\circ$ ,  $\sigma_L$  must be less than  $0.01m$ , probably about  $0.005m$ .

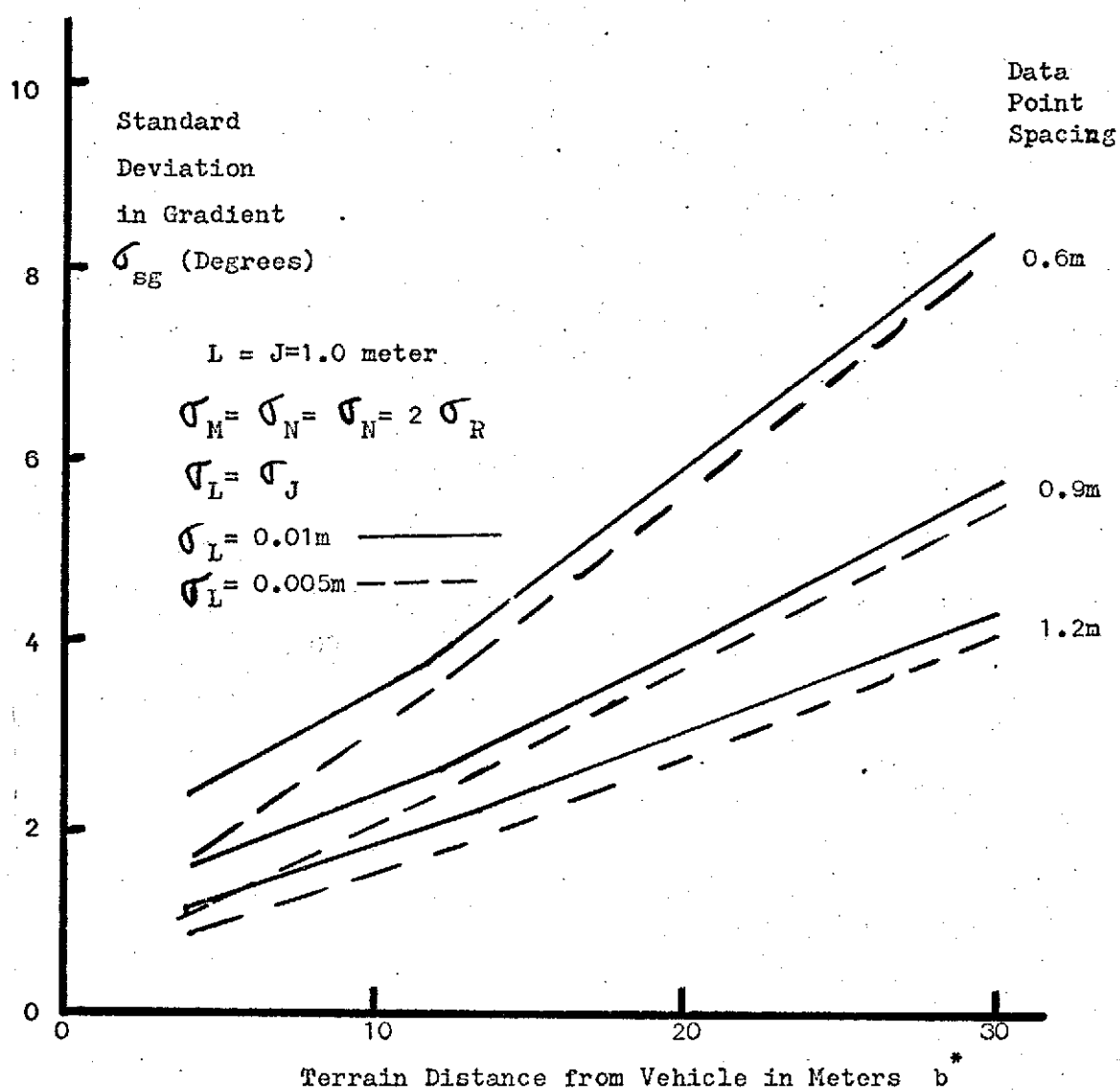


Figure 9 Stereo Range System: Standard Deviation in Gradient Versus Terrain Distance from Vehicle with Relative Slope = 0

At longer range, data point spacing should be increased to a value greater than one meter. For example, at 20 meters either the spacing must be greater than 1.2 meters or the range standard deviation  $\sigma_R$  must be reduced below 0.001m in order to obtain a value of  $\sigma_{sg}$  to be less than 2 degrees.

Figure 10 is a plot of the standard deviation in gradient vs. relative in-path slope at a distance of 4 meters from the vehicle having data point spacing of 0.6m. The range of relative in-path slopes is from  $-27^\circ$  to  $+50^\circ$  for the same reasons as for the stereo angles system. In this case  $\sigma_{sg}$  decreases as relative in-path slope increases to  $+50^\circ$ . From the figure it is concluded that to obtain the value of  $\sigma_{sg}$  to be less than  $2^\circ$  for most relative in-path slopes, the magnitude of  $\sigma_R$  must be 0.001m or less and the magnitude of  $\sigma_L$  must be 0.005m or less.

In Figure 11 the standard deviation in gradient is plotted against relative in-path slopes at a distance of 20 meters with data point spacing of 1.2 meters. In this graph the value of the quantity  $\sigma_{sg}$  increases slightly as relative in-path slope increases to  $+50^\circ$ . To obtain a maximum standard deviation  $\sigma_{sg}$  of  $2^\circ$  when the value of  $\sigma_L$  is 0.005m, the range standard deviation  $\sigma_R$  must be about 0.0005m.

Figure 12 shows the standard deviation in gradient versus relative cross-path slopes from  $0^\circ$  to  $50^\circ$  at 4 and 20 meters with data point spacings of 0.6m and 1.2m respectively. The quantity  $\sigma_R$  is 0.001m and  $\sigma_L$  is 0.01m and 0.005m. Again the value of  $\sigma_R$  must be less than 0.001m in order to obtain relatively small standard deviation in gradient.

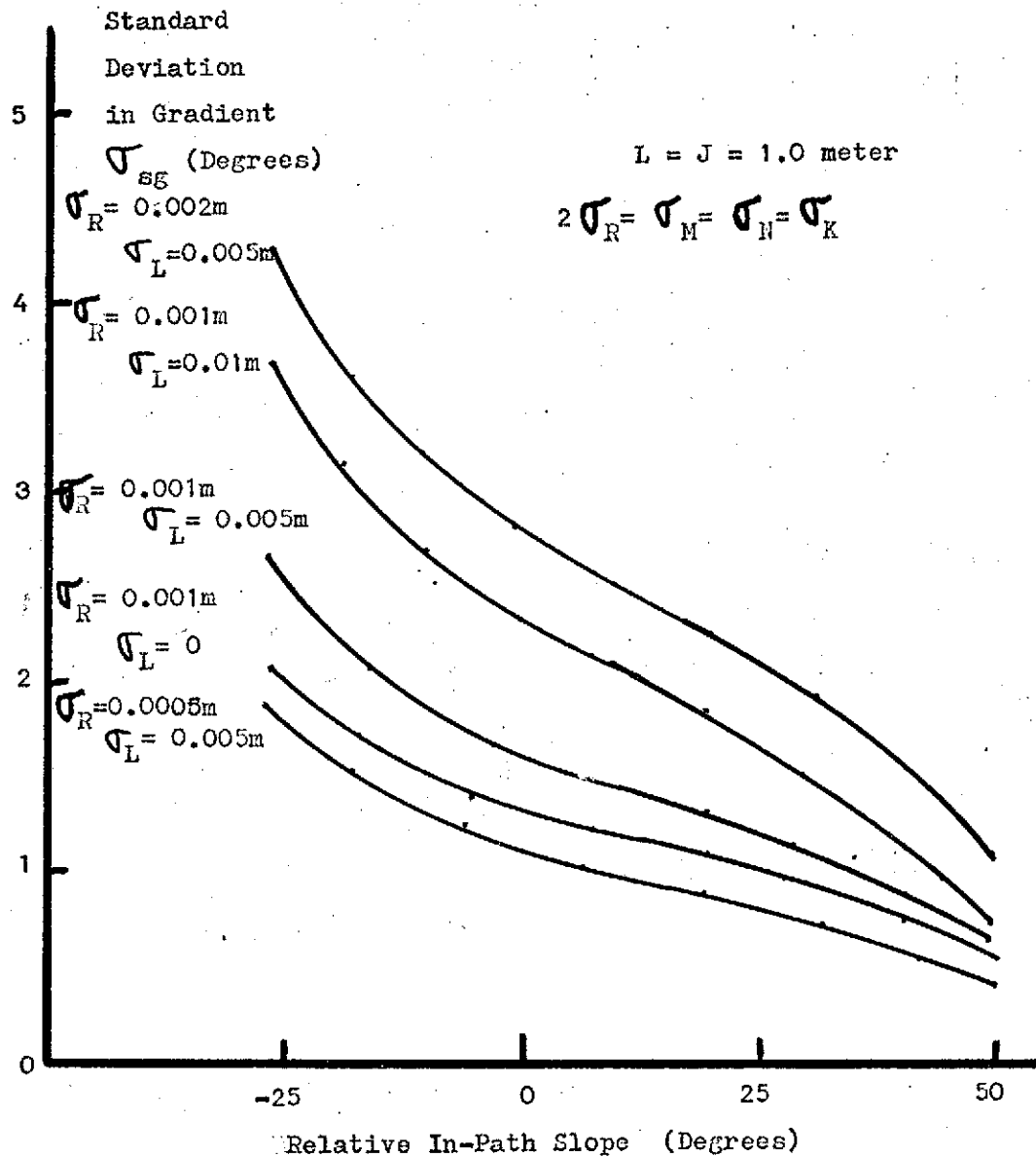


Figure 10 Stereo Range System: Standard Deviation in Gradient Versus Relative In-Path Slope for Terrain at 4m with Point Spacing = 0.6m



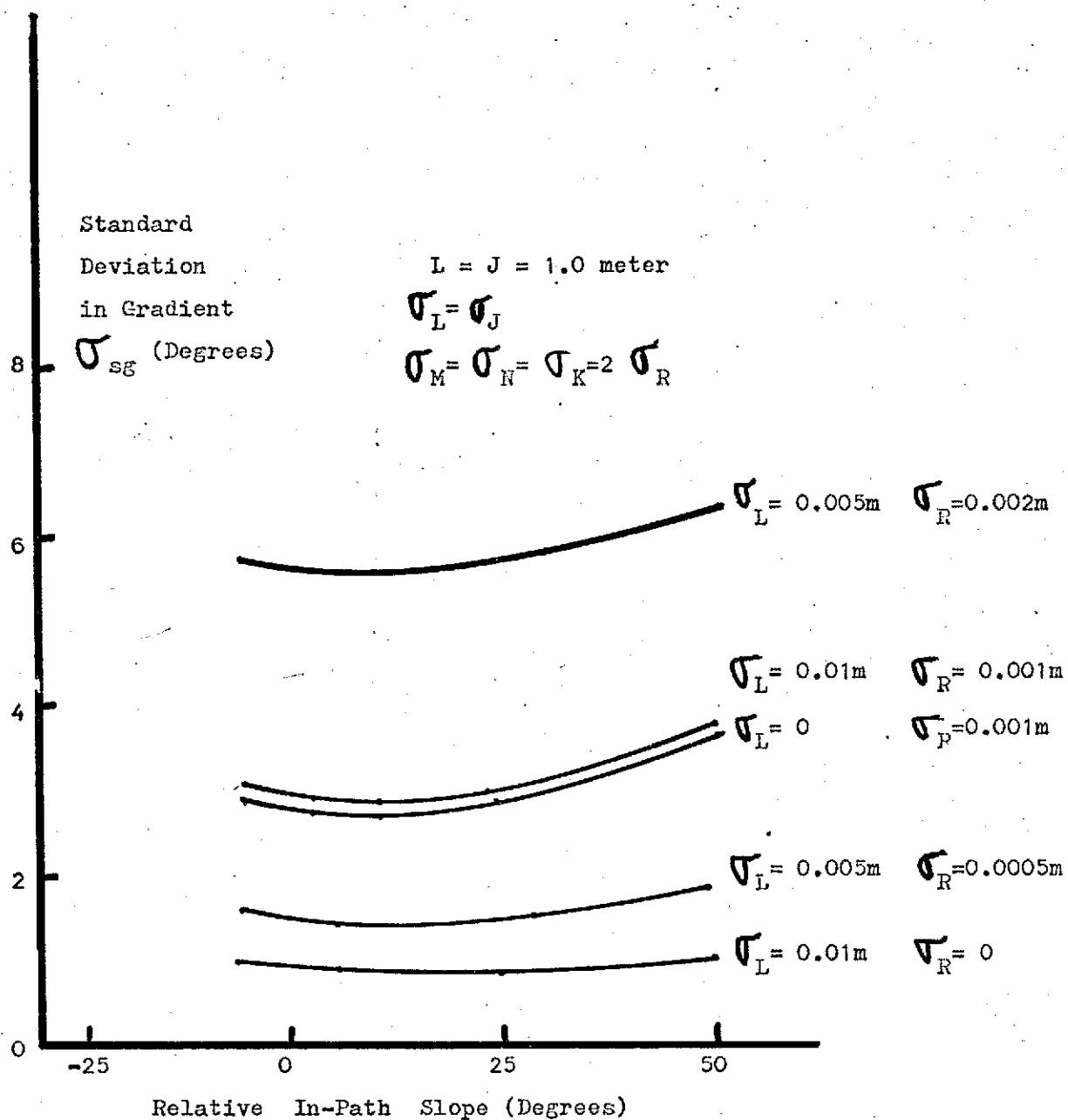


Figure 11 Stereo Range System: Standard Deviation in Gradient Versus  
Relative In-Path Slope for Terrain at 20m with Point Spacing = 1.2m

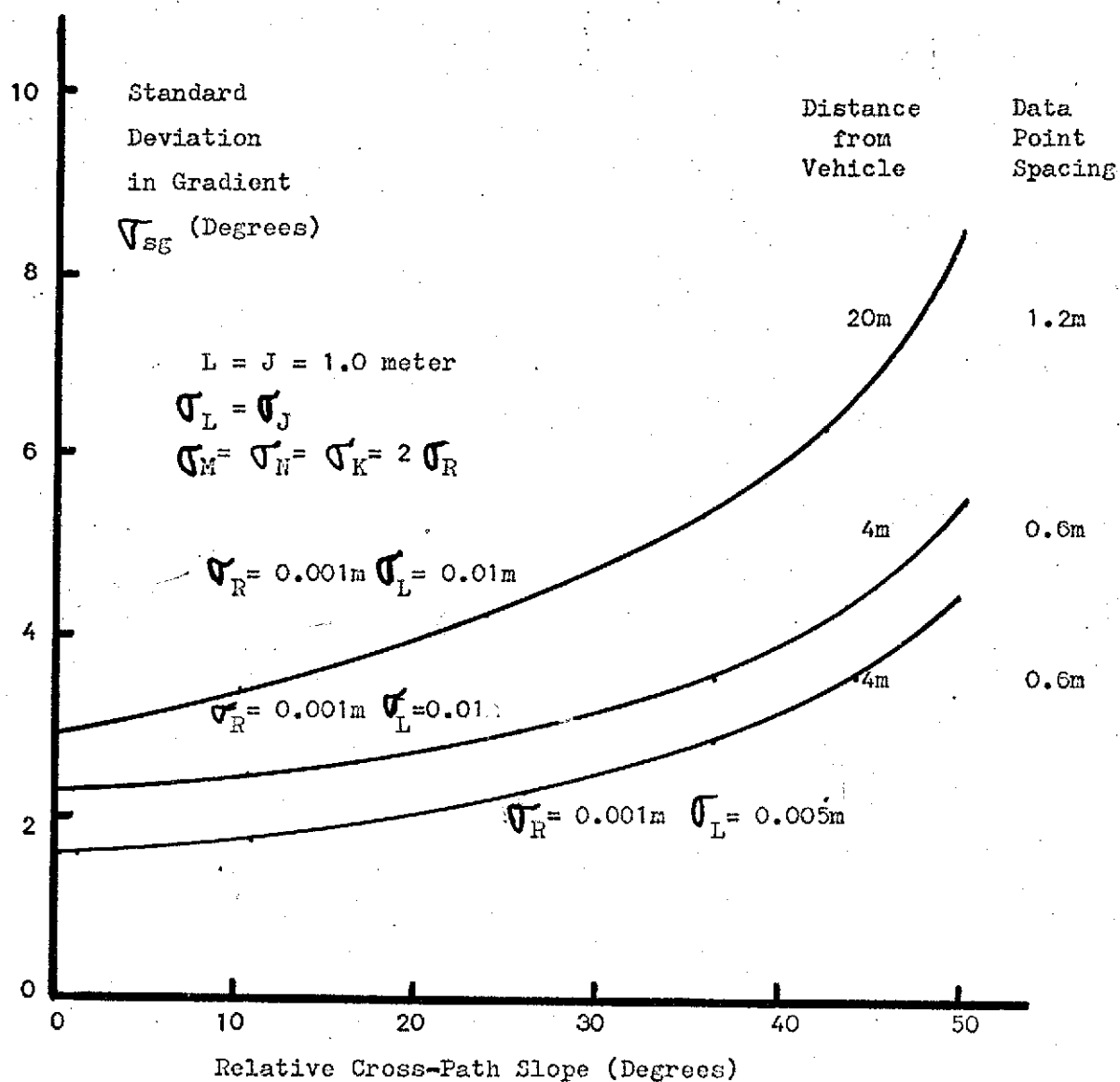


Figure 12 Stereo Range System: Standard Deviation in Gradient Versus Relative Cross-Path Slope for Terrain at 4 and 20 Meters

### 3. Comparisons of the Four Point Fit with a Three Point Fit

The gradient of the terrain may be estimated by modeling a plane containing three data points. Since 3 points determine a plane the sum in Eq. (9) reduces to zero. From the three point plane the cross-path slope,  $\bar{x}_1$ , and the in-path slope,  $\bar{x}_2$ , and their covariances are calculated in Eqs. (11) and (22). These results are used in Eq. (25) to compute a standard deviation in gradient  $\sigma_{sg}$ .

Comparisons of the accuracy of the gradient estimate for the three and four point schemes are shown in Figures 13-16. Fig. 13 shows the quantity  $\sigma_{sg}$  vs. relative in-path slope at 4 meters for the stereo angles system with point spacing of 0.6m. For relative in-path slopes less than about  $10^\circ$  the 4 point fit is much more accurate. This is important since over much of its course the vehicle will be measuring terrain with relative slope in the  $-20^\circ$  to  $+20^\circ$  range.

The next graph (Fig. 14) shows  $\sigma_{sg}$  plotted against relative in-path slope at 20 meters distance with point spacing equal to 1.2m. In this case the four point stochastic fit is better than the 3 point method for all relative slopes.

Figures 15 and 16 show the comparison for the stereo range system at 4 and 20 meters respectively. At close range a 4 point fit is much more accurate for positive relative in-path slopes. At 20 m the four point stochastic estimate is considerably more accurate than the three point calculation for all relative in-path slopes.

Since the calculation in the 3 point case is nearly as complicated as the four point case and the resulting estimate of gradient is much less accurate with a 3 point system, the four point

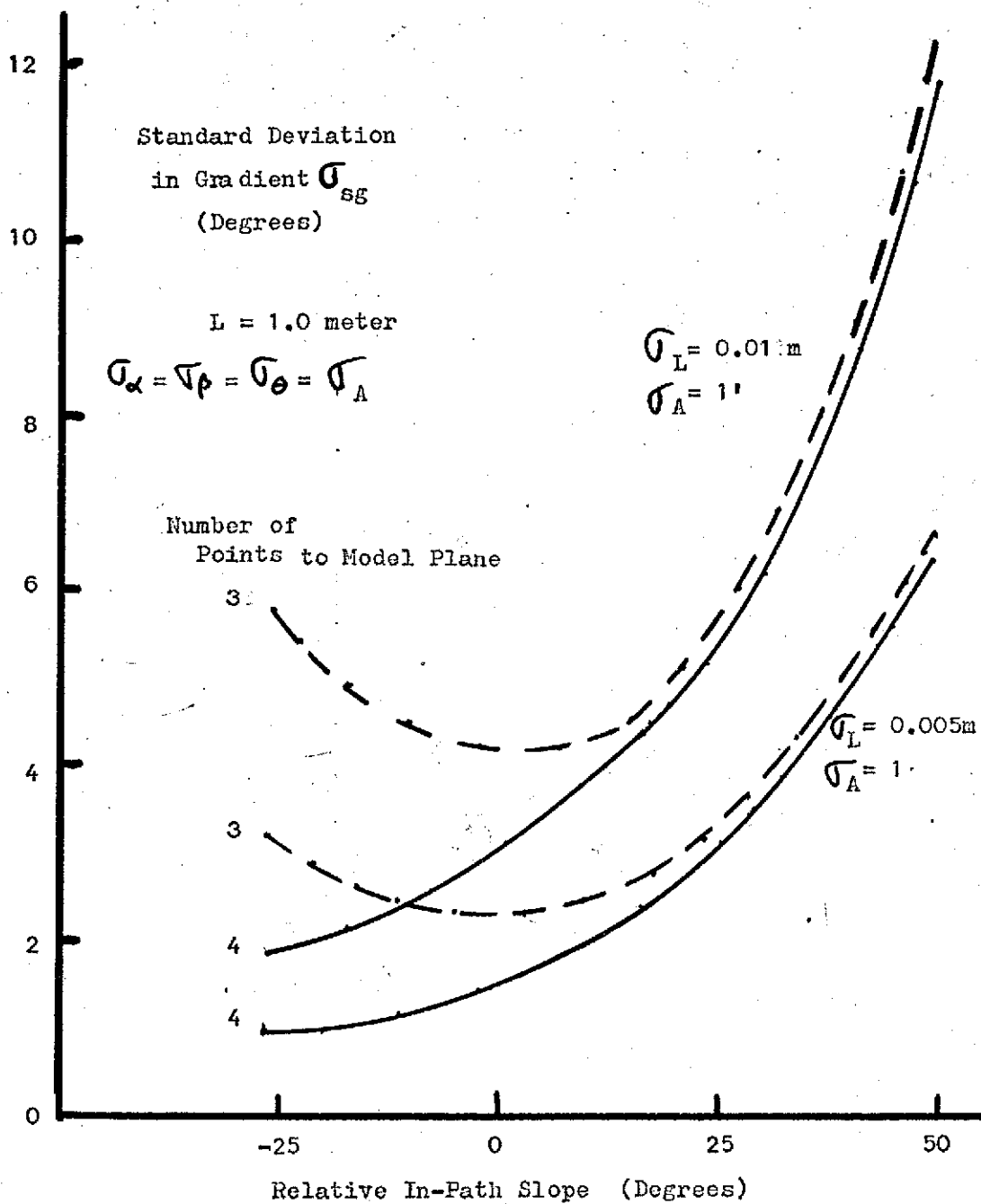


Figure 13 Stereo Angles System: Standard Deviation in Gradient Versus  
Relative In-Path Slope at 4 Meters with Point Spacing = 0.6m  
for 3 and 4 Point Planes

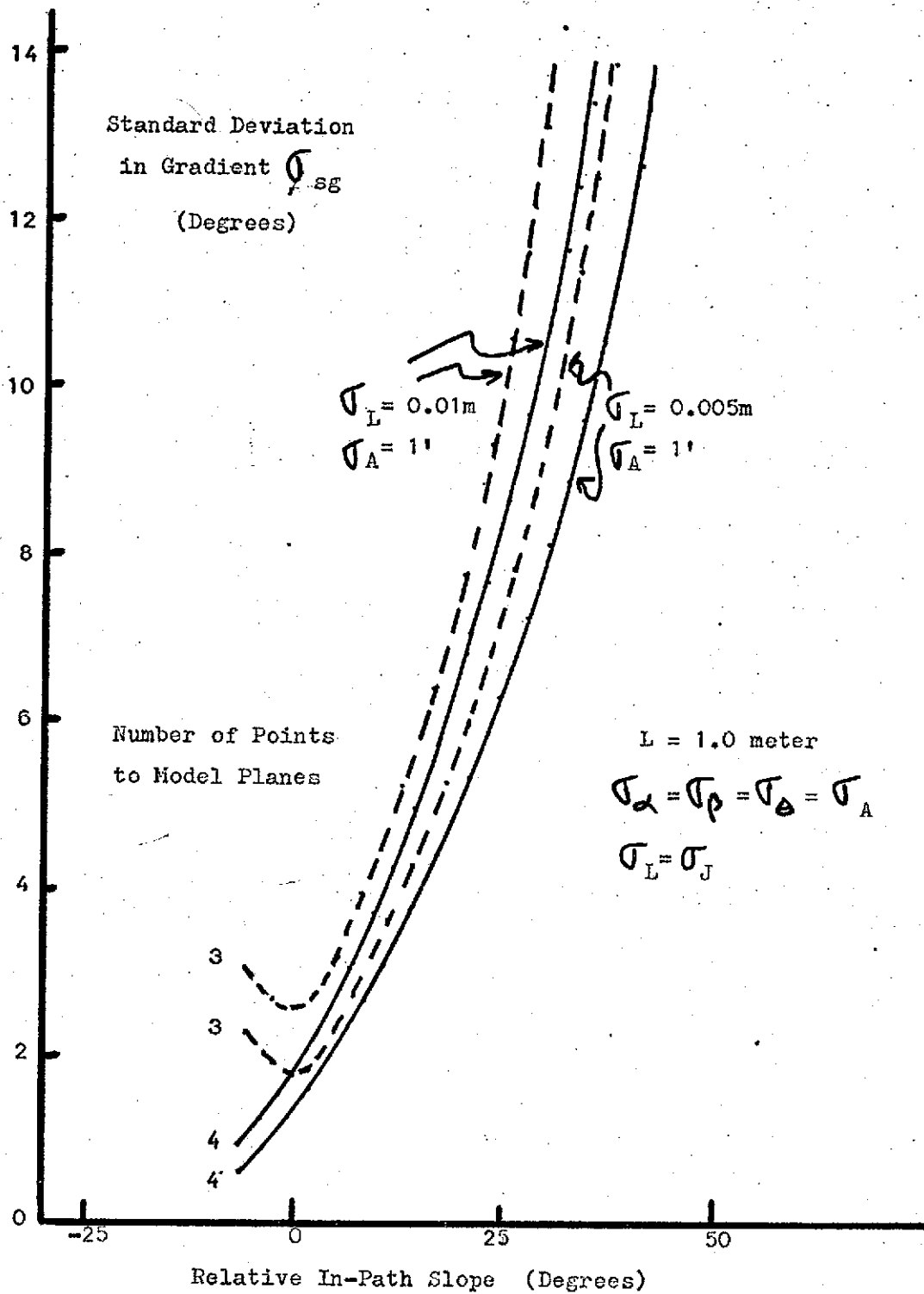


Figure 14 Stereo Angles System: Standard Deviation in Gradient Versus  
Relative In-Path Slope at 20 meters with Point Spacing = 1.2m  
for 3 and 4 Point Planes

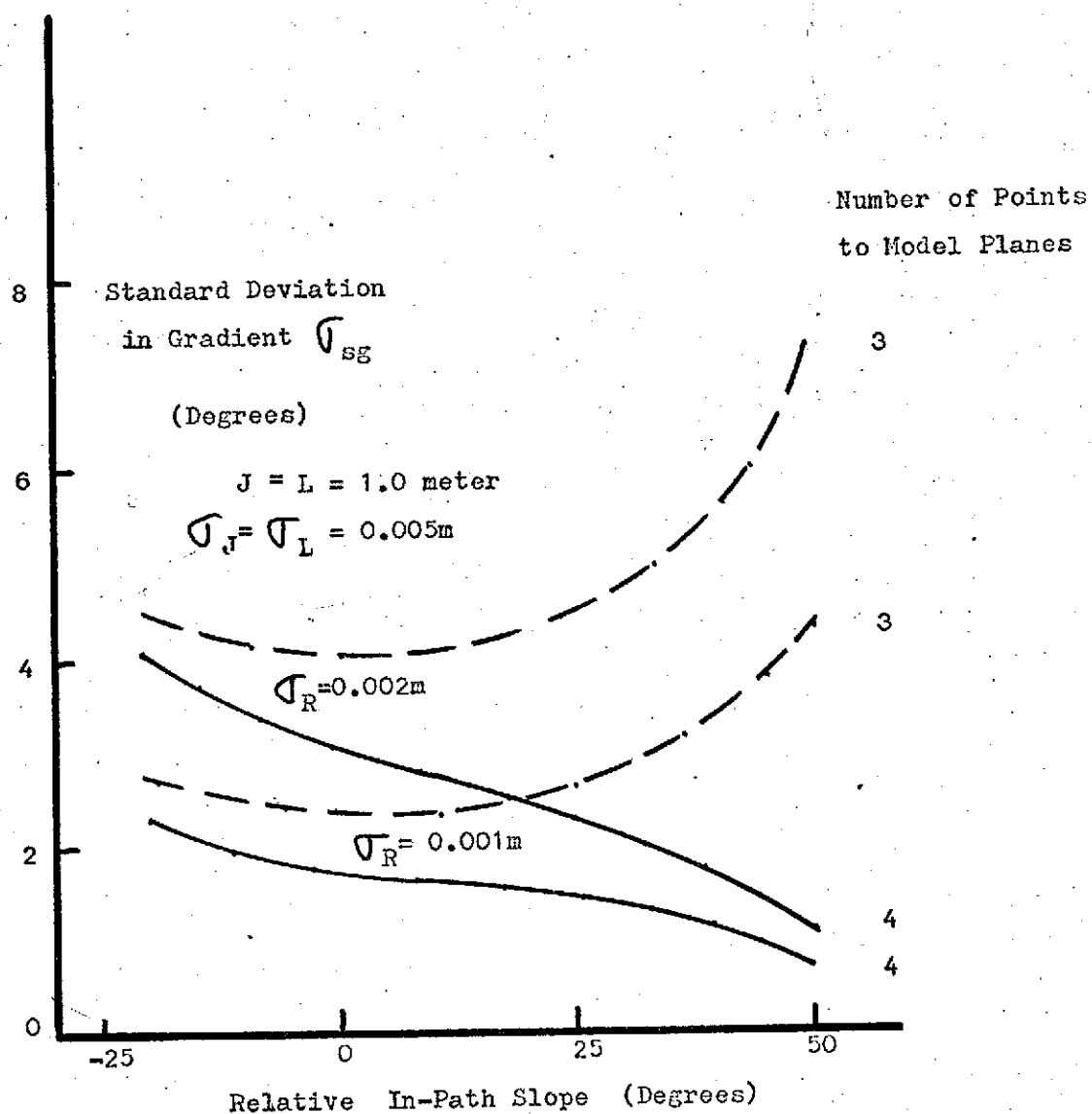


Figure 15 Stereo Range System: Standard Deviation in Gradient Versus  
Relative In-Path Slope at 4 meters with Point Spacing = 0.6m  
for 3 and 4 Point Planes

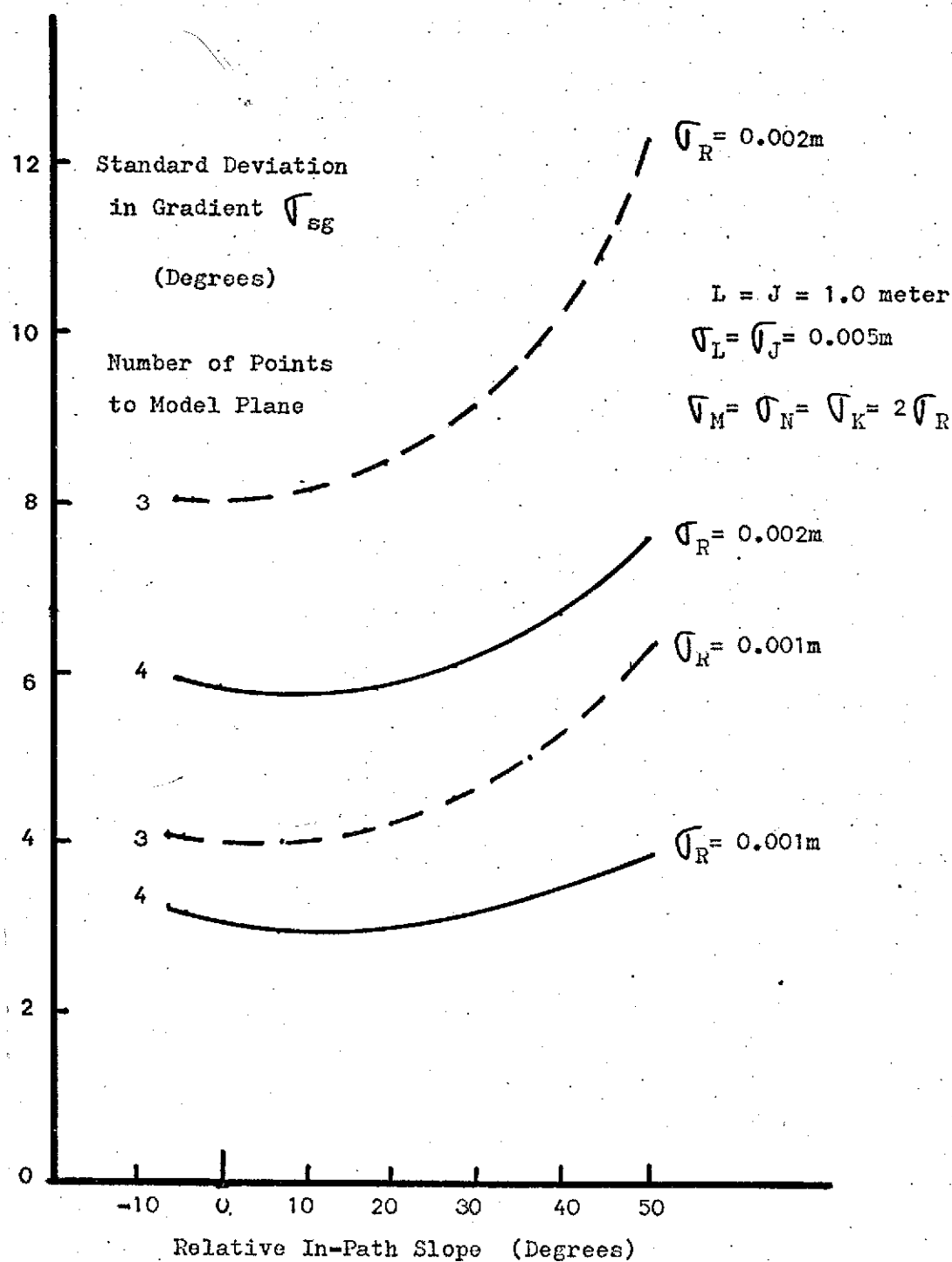


Figure 16 Stereo Range System: Standard Deviation in Gradient Versus Relative In-Path Slope at 20 meters with Point Spacing = 1.2m for 3 and 4 Point Planes

stochastic estimate is clearly recommended.

#### 4. Standard Deviations in $h'$ , $a'$ and $b'$

The standard deviations in  $h'$ ,  $a'$  and  $b'$  may be determined from Eq. (15). Since these uncertainties are involved in the estimate of the gradient a closer look at these parameters may explain some of the results previously discussed. It is also possible that the path selection algorithm may take height differences between data points into account. [1]

The standard deviation in the coordinate  $h'$  is plotted against distance from the vehicle for the stereo angles system in Figure 17. The value of  $L$  is one meter and its standard deviation is 0.01m. The terrain assumed is flat with zero height and no relative slope. Since the critical height for path selection may be about .45 meter the standard deviation in the height measurement should be no more than a few centimeters. From the figure it is obvious that the angle standard deviation should be about 1". Reducing the quantity  $\sigma_A$  to 6" give little improvement in the accuracy of the measurement of the coordinate  $h'$ . Figure 18 shows the effects of the separation standard deviation on the height uncertainty  $\sigma_h$ . In this case the terrain is again assumed to be flat with zero height and no relative slope.

The standard deviation in the coordinate  $a'$  is slightly less than the standard deviation in  $h'$  for all cases with the stereo angles system. The standard deviation in  $b'$ , as shown in Figure 19, is very large for the stereo angles system. The inaccuracy in the measurement of the coordinate  $b'$  increases rapidly as distance from the vehicle increases. If accurate discrete point locations are needed the stereo



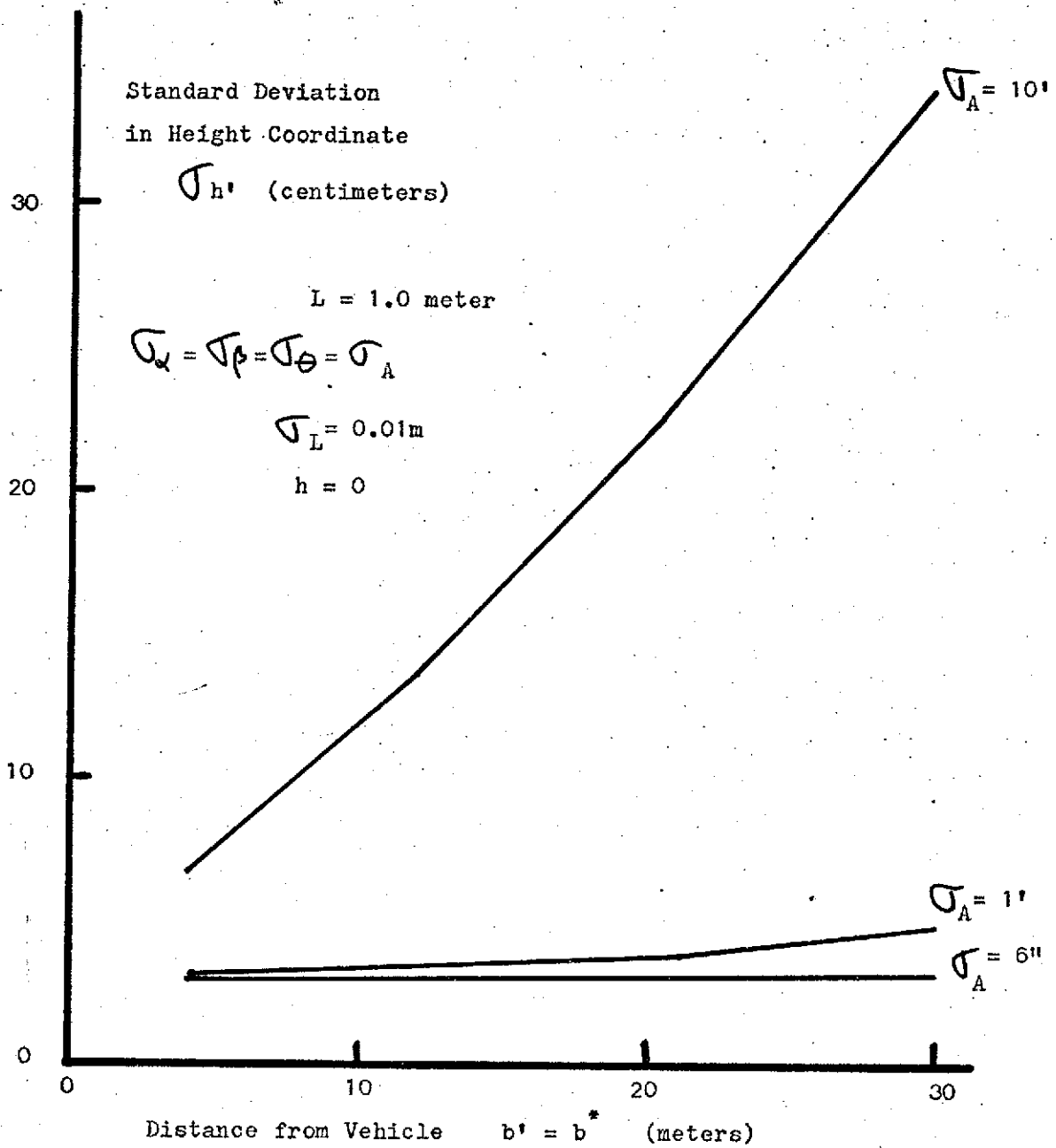


Figure 17 Stereo Angles System: Standard Deviation in Height Coordinate ( $h'$ ) Versus Distance from Vehicle for Flat Terrain with  $h'=0$

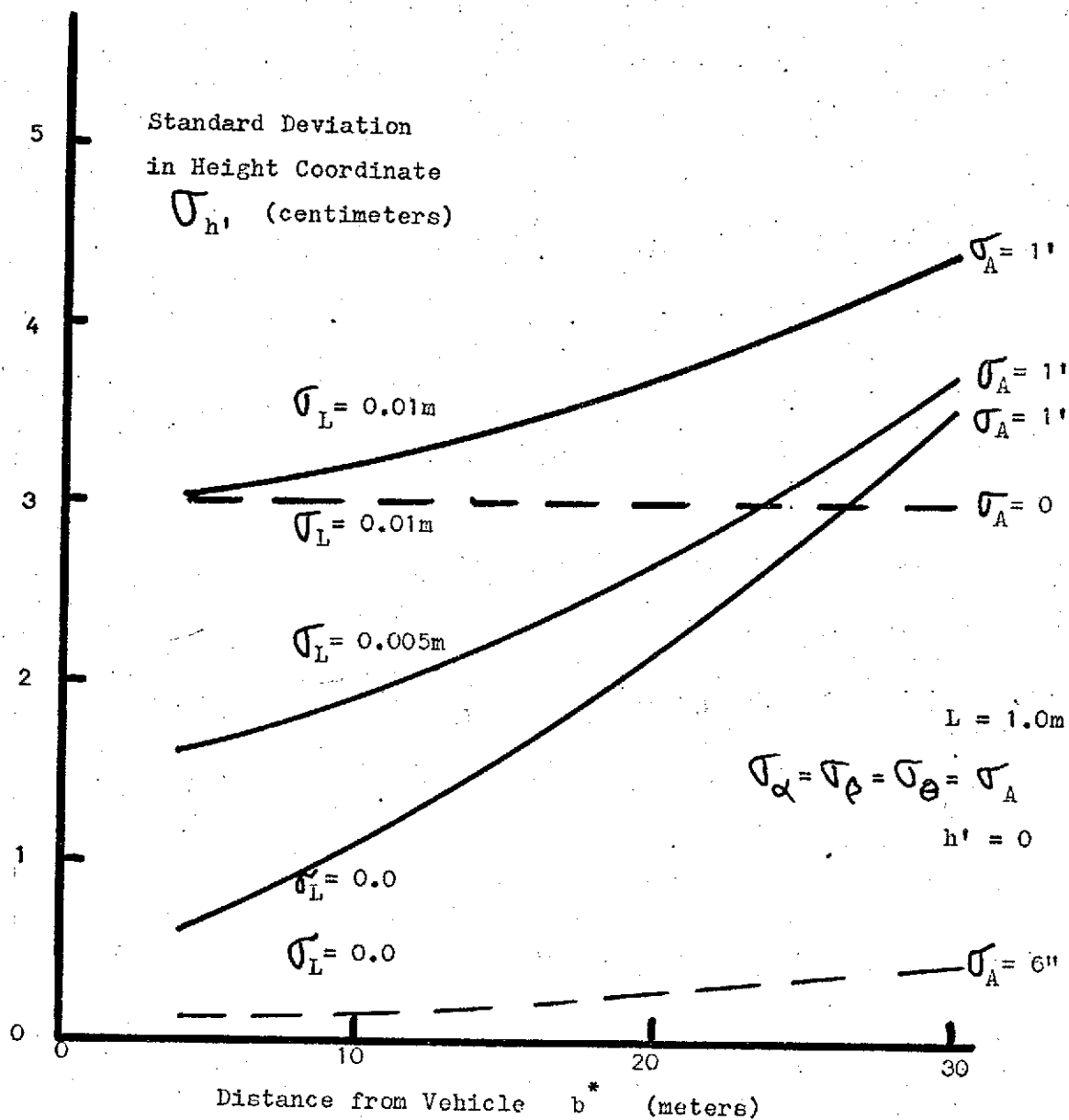


Figure 18 Stereo Angles System: Standard Deviation in Height Coordinate ( $h'$ ) Versus Distance from Vehicle for Flat Terrain with  $h'=0$

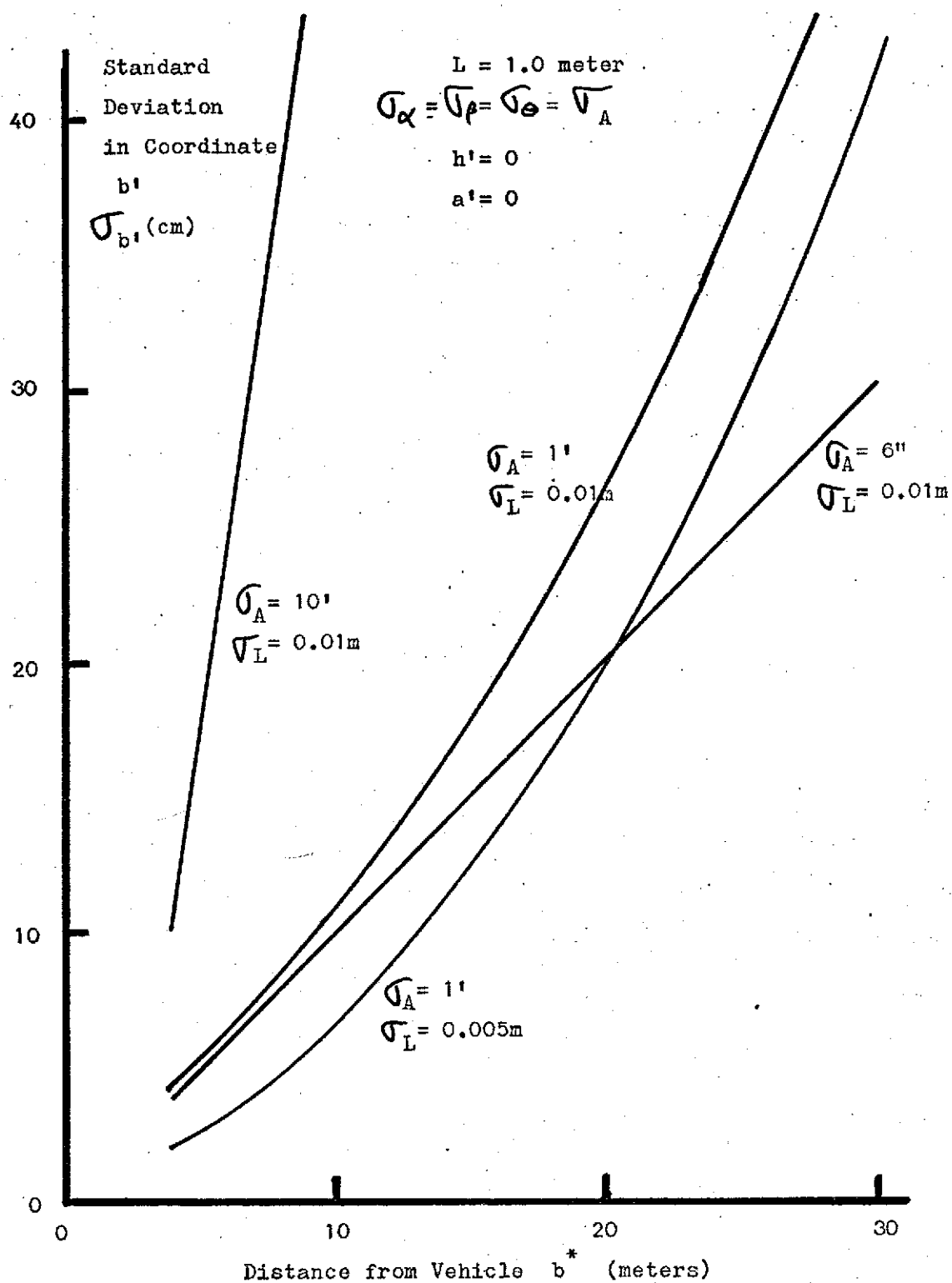


Figure 19 Stereo Angles System: Standard Deviation in Coordinate  $b'$   
 Versus Distance from Vehicle for Flat Terrain with  $h' = 0$

might be restricted to use only at close range, say within 10-15 meters. Heights of terrain other than zero have a noticeable but tolerable effect on the measurement of  $h$  as shown in figure 20. This graph shows the quantity  $\sigma_h$  vs. distance  $b^*$  for  $h' = +1, 0$  and  $-1$  meter when  $L = 1.0m$ ,  $\sigma_L = 0.01m$  and  $\sigma_A = 1'$ . The system is more accurate for positive heights than for negative heights. The measurements of  $a'$  and  $b'$  are not sensitive to the variation in height.

The stereo range system requires very good range accuracy to obtain good  $h'$  coordinate accuracy as seen from Figure 21, standard deviation in height  $h'$  vs. distance  $b^*$ . The separation uncertainty has much less effect than the range uncertainty. To get accurate results the range standard deviation must be 0.001 meter or less. Figure 22 shows the quantities  $\sigma_{a'}$  and  $\sigma_{b'}$  vs. distance for the stereo range system. The accuracy in the  $a'$  coordinate is about the same as in the  $h'$  coordinate because of the symmetry of the system. The standard deviation  $\sigma_{b'}$  is small and should pose no problem for this system. Figure 23 illustrates the effects of heights of terrain not equal to zero on the accuracy of the stereo range system. The measurement of  $a'$  is not sensitive to height variation. The measurements of the values of  $h'$  and  $b'$  are slightly affected by terrain height variation.

The standard deviations in the coordinates  $h'$ ,  $a'$  and  $b'$  are plotted versus distance from the vehicle for the non-stereo system in Figures 24-26. This system differs from the stereo systems in that when angle standard deviation is  $1'$  the standard deviation in  $h'$ ,  $\sigma_h$ , decreases considerably as the distance from the vehicle increases. There is some threshold value for the quantity  $\sigma_A$  between  $1'$  and  $10'$

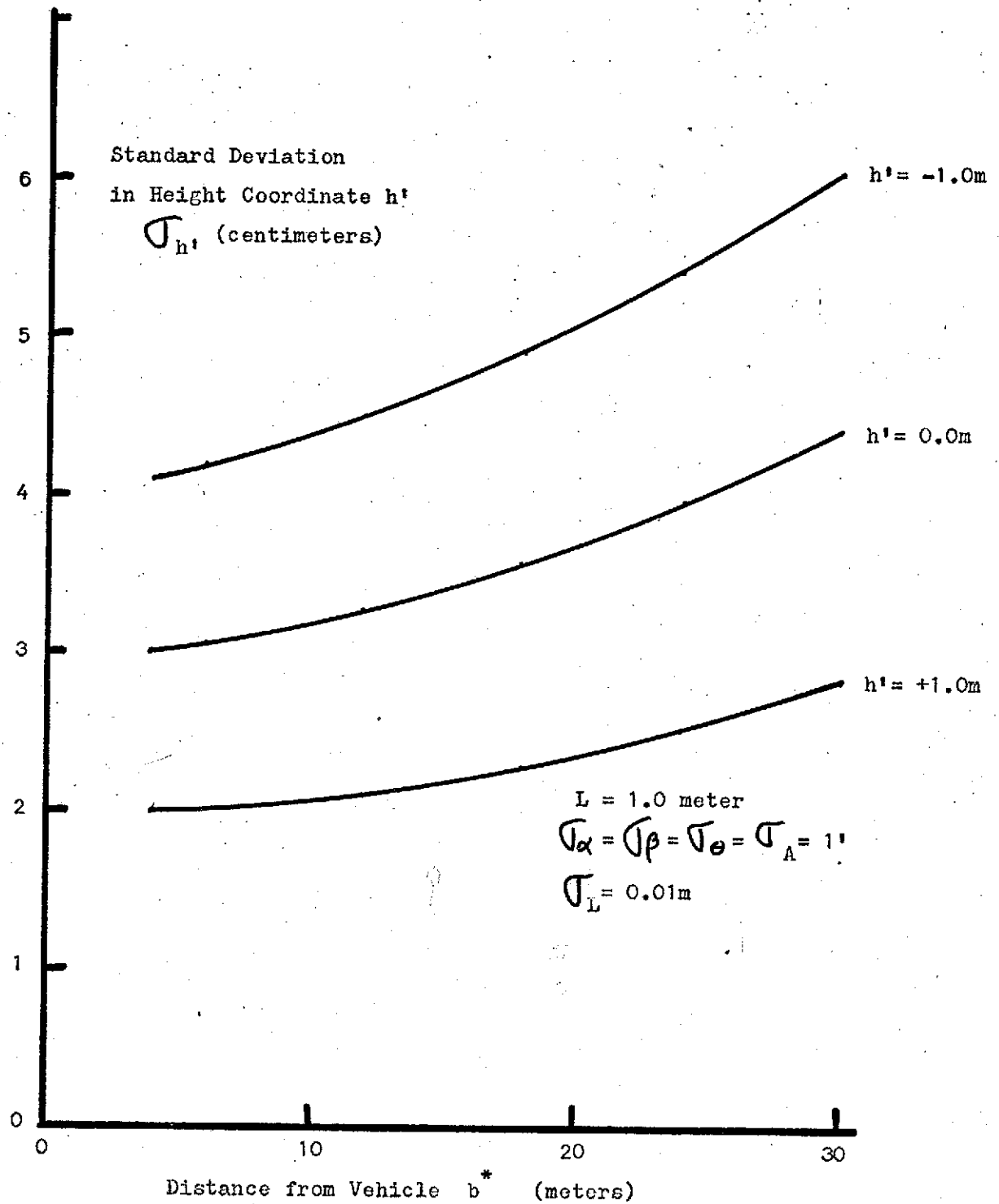


Figure 20 Stereo Angles System: Standard Deviation in Height Coordinate  $h'$   
Versus Distance from Vehicle for Various Values of  $h'$

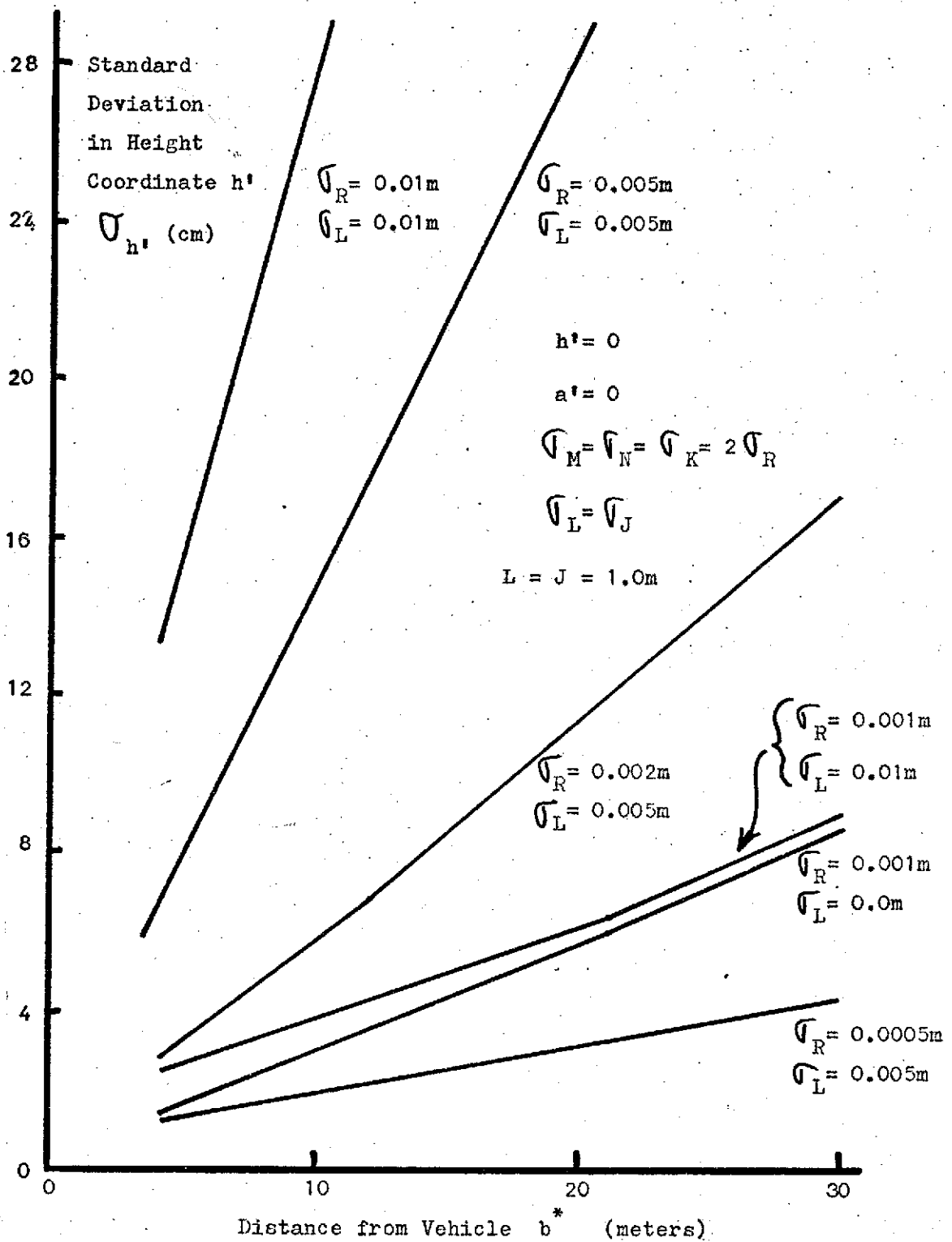


Figure 21 Stereo Range System: Standard Deviation in Height Coordinate  $h'$   
 Versus Distance from Vehicle for Flat Terrain with  $h' = 0$

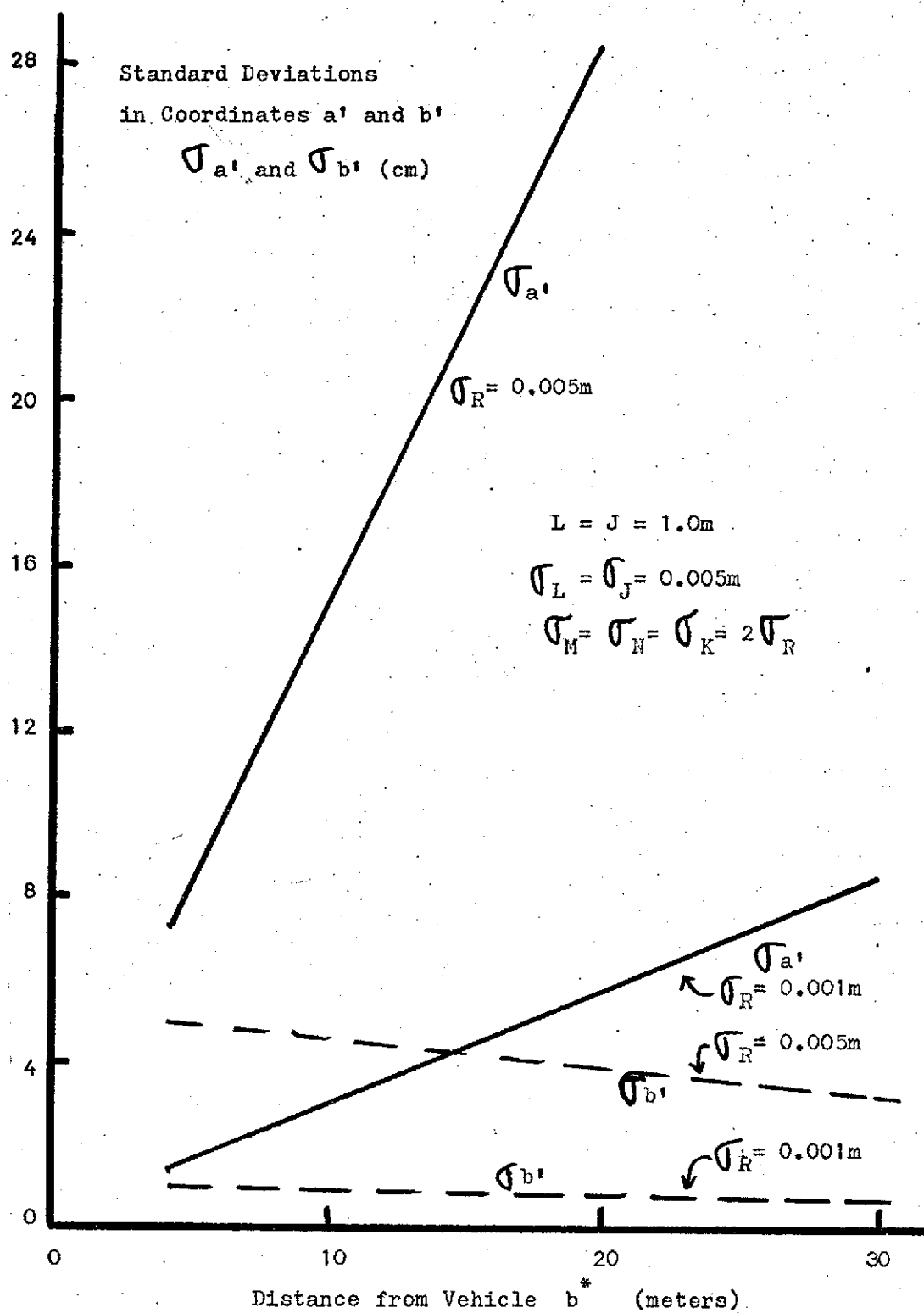


Figure 22 Stereo Range System: Standard Deviations in  $a'$  and  $b'$  Coordinates  
Versus Distance from Vehicle for Flat Terrain with  $h' = 0$

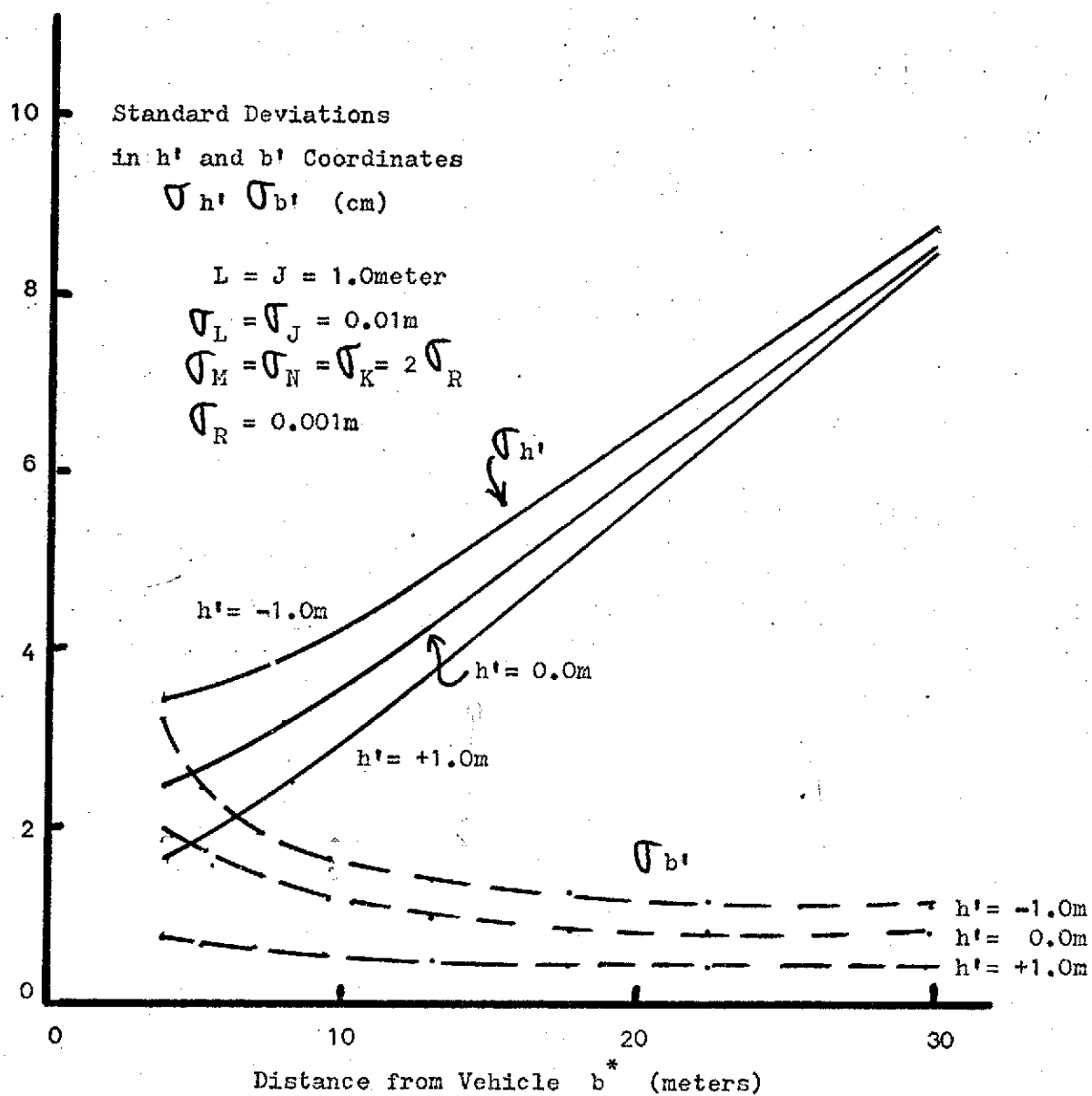


Figure 23 Stereo Range System: Standard Deviations in  $h'$  and  $b'$  Coordinates  
Versus Distance from Vehicle for Various Values of  $h'$



above which this effect is reversed. At close range with angle standard deviation equal to  $1'$  the range uncertainty appears dominant. A value of  $\sigma_R = 0.05\text{m}$  or less will give acceptable results in the measurement of  $h'$  if the value  $\sigma_A = 1'$ . For the non-stereo system the magnitude of the standard deviation in the coordinate  $a'$  is always less than the standard deviation in  $h'$ .

The standard deviation in the measurement of the  $b'$  coordinate vs. distance from the vehicle is illustrated in Figure 25. The angular standard deviation is  $1'$  for the solid lines and  $10'$  for the dotted lines. The range standard deviation  $\sigma_R$  varies from  $0.01\text{m}$  to  $0.10\text{m}$ . The terrain is assumed to be flat with zero height. The uncertainty in  $b'$  is approximately equal to the range standard deviation. Again the measurements of  $a'$  and  $b'$  are not significantly influenced by changes in the height  $h'$ . The effect of heights from  $+1\text{meter}$  to  $-1\text{meter}$  on the quantity  $\sigma_{h'}$  are shown in Figure 26. Angle standard deviation is set at  $1'$  and range standard deviation at  $0.10\text{m}$ . As with the other systems the effects of non-zero heights is acceptable.

The fact that the accuracy in the coordinate measurements improves with increasing distance from the vehicle for the non-stereo system explains why gradient estimates also improve with distance for this system as shown in the literature.<sup>[2]</sup>

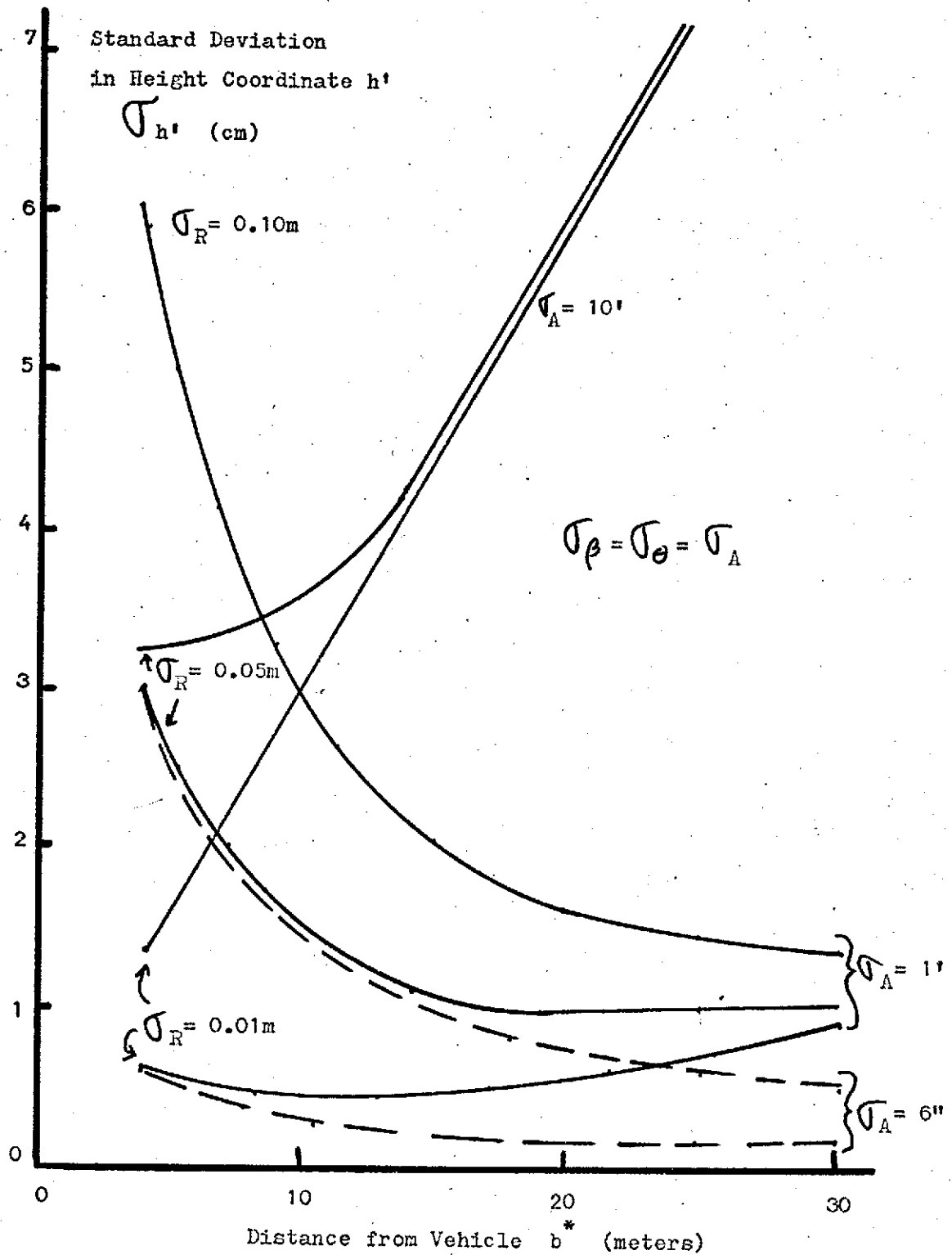


Figure 24 Non-Stereo System: Standard Deviation in Height Coordinate  $h'$   
Versus Distance from Vehicle for Flat Terrain with  $h' = 0$

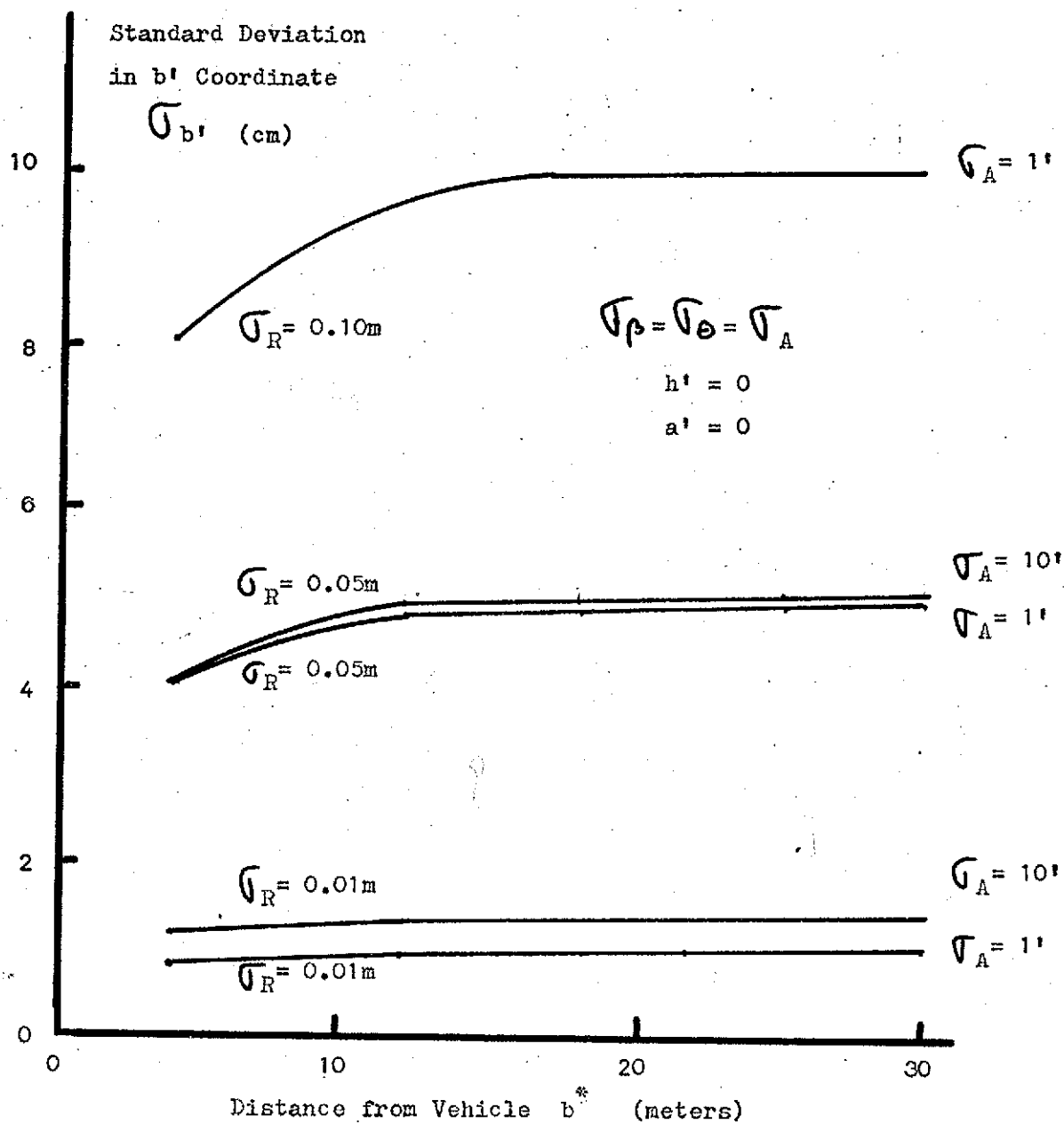


Figure 25 Non-stereo System: Standard Deviation in  $b'$  Coordinate  
Versus Distance from Vehicle for Flat Terrain with  $h' = 0$

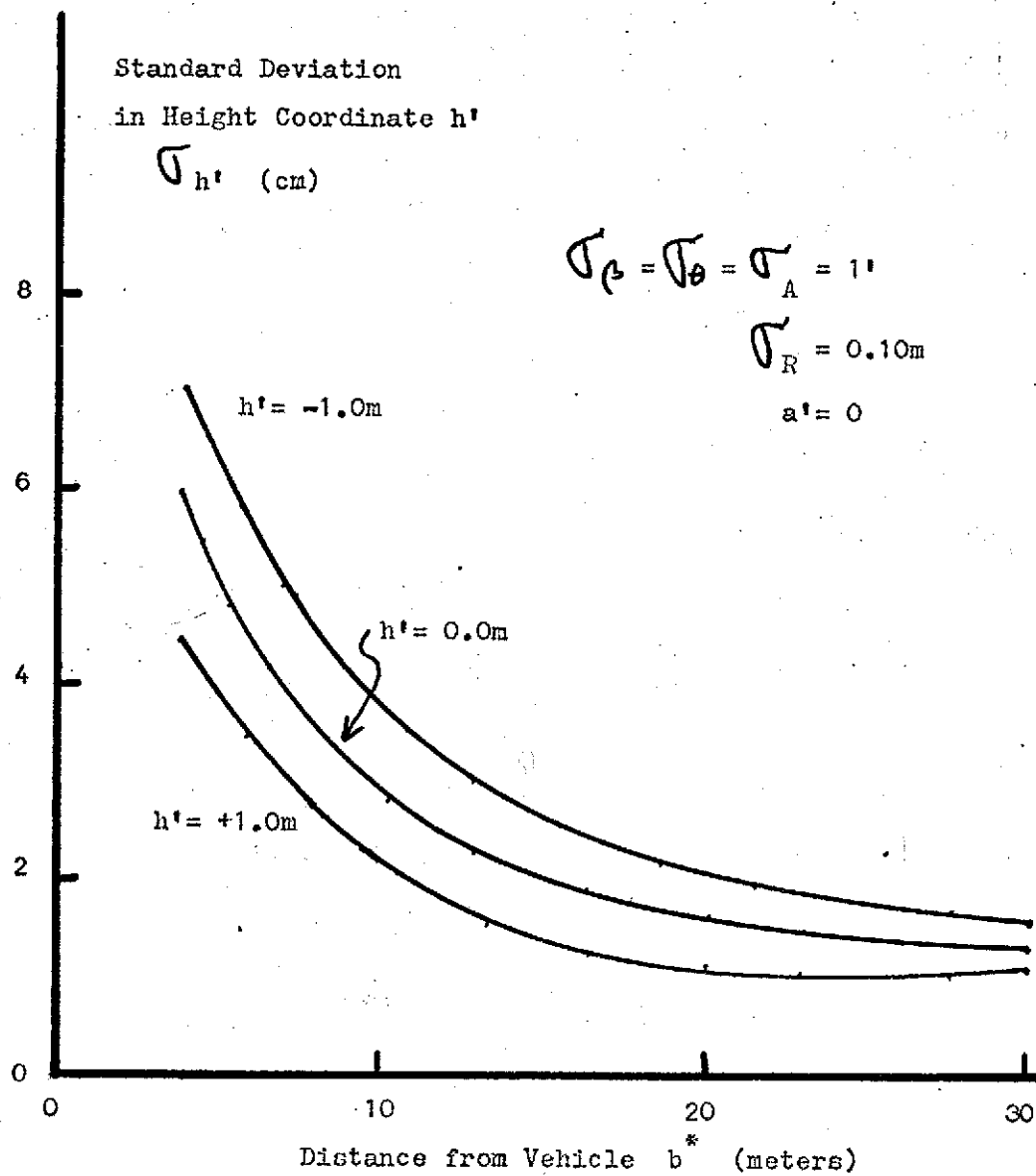


Figure 26 Non-stereo System: Standard Deviation in Height Coordinate  $h'$   
Versus Distance from Vehicle for Various Values of  $h'$

PART 5  
CONCLUSIONS

A procedure for estimating a state vector  $x$  from the relation  $h = A x$  when  $h$  and  $A$  are stochastic measurements has been applied to estimate the gradient of the terrain in the path of the Martian vehicle. Four measurement points which do not lie on the same plane due to terrain irregularities and measurement errors are employed to form a least square estimate of the gradient. This least square estimate has been found to be more accurate than an estimate from only three points which lie on the plane.

The standard deviation in the four point estimate of the gradient depends on the distance of the four points from the vehicle, the positions of the terrain points in relation to each other, the gradient of the terrain and the measurement errors. Vehicle motion effect on the standard deviation in gradient has been reduced to an additive factor as a result of use of a rapid-scan laser.

The effects of the above factors on the quantity  $\sigma_{sg}$  are shown in Figures 5-8 for a stereo angles measurement system which uses 3 angular measurements and in Figures 9-12 for a stereo range system which uses 3 range measurements. A desired maximum allowable standard deviation in gradient  $\sigma_{sg}$  has been set at  $2^\circ$ . These results are summarized and compared with the non-stereo system which uses one range and two angular measurements, [1,2] in the following Table.

TABLE

COMPARISON OF STEREO AND NON-STEREO  
MEASUREMENTS USING FOUR POINT PLANE FITTING

SYSTEM	MAX. RANGE STD. DEV. $\sigma_R$	MAX. ANGLE STD. DEV. $\sigma_A$	MAX. DISTANCE L & J STD. DEV. $\sigma_L = \sigma_J$
At 4 meters from the vehicle:			
Stereo Range	0.001 meter	-----	0.005 meter
Stereo Angles	-----	1 minute	0.001 meter
Non-stereo	0.01 meter	1 minute	-----
At 20 meters from the vehicle:			
Stereo Range	0.0005 meter	-----	0.005 meter
Stereo Angles	-----	6 arc-sec.	0.001 meter
Non stereo	0.02-0.03 meter	1 minute	-----

From the Table and the limits of present technology, the non-stereo system appears much more practical than the stereo range system. Laser rangefinder technology has not yet reduced range standard deviation  $\sigma_R$  below 0.01 meter.<sup>[3]</sup> In fact, a more reasonable expectation for range standard deviation may be from 0.02 to 0.05m.<sup>[12]</sup> The results for stereo range have been presented in anticipation of improvements in rangefinder accuracy.

At longer range the non-stereo system is better than the stereo angles system. At close range, stereo angles may be comparable to non-stereo if the standard deviation in the transmitter-receiver separation  $\sigma_L$  can be reduced to 0.001m. This conclusion is also based on the assumption that angle standard deviation will be about one minute of arc. [3]

Future research should consider the problem of coordinating the gradient estimates of all the small terrain areas in front of the vehicle. The problem of discrete obstacle detection or height discontinuities should also be analyzed. A complete path selection rule should then be developed and tested. Other possibilities include rearrangement of transmitter and receivers to improve accuracy and simplify operation of the obstacle detection system.

PART 6  
REFERENCES

1. Golden, J., "An Obstacle Detection System for Mid-Range Path Selection for an Autonomous Roving Vehicle", R.P.I. Masters Project Report, June 1972.
2. Shen, C.N., & Burger, P., "Stochastic Estimates of Gradient from Laser Measurements for an Autonomous Martian Vehicle", proceedings of the IFAC Symposium on Identification and Estimation at Hague, The Netherlands, June 1973.
3. Palumbo, D., "Design of Laser Rangefinder for Terrain Modeling", semi-annual report to NASA; R.P.I. Troy, New York, February 1973.
4. Fox, E.A., MECHANICS, Harper & Row, New York, 1967, p.237.
5. Pavarini, C. and Chrysler, J.H., "Terrain Modeling and Path Selection by an Autonomous Martian Exploratory Vehicle", R.P.I. Technical Report MP-14, NASA Grant 33-018-191, June 1970.
6. Rautio, A., "An Analysis of Effect of Sensor Errors on a Long Range Terrain Modeling System and a Study of Short Range Terrain Modeling for an Autonomous Roving Vehicle", R.P.I., Masters Project Report, June 1971.
7. DeRusso, P., Roy, R., and Close, C., STATE VARIABLES FOR ENGINEERS, John Wiley & Sons, Inc., New York, 1965, pp. 457-461.
8. Bryson, A.E. and Ho, Y.C., APPLIED OPTIMAL CONTROL, Ginn-Blaisdell Publishing Co., 1969, Chapter 12.
9. Shen, C.N., "Random Variables, Gauss-Markov Random Sequences and Linear Discrete Optimal Filtering", unpublished notes, R.P.I., Troy, N.Y.
10. Bevington, P., DATA REDUCTION AND ERROR ANALYSIS FOR THE PHYSICAL SCIENCES, McGraw-Hill Co., New York 1969, p.59.
11. Herb, G., "Terrain Sensor Instrumentation- Laser Scan Methods", semi-annual report to NASA; R.P.I., Troy, New York, February 1973.
12. Zuraski, G., "Range Measurement", annual report to NASA; R.P.I., Troy, New York, May 1972.



## APPENDIX A

### Derivation of the Perturbation Equations

To prove the results in Eqs. (12) and (13) the  $h$ ,  $a$ ,  $b$  coordinates are first perturbed as

$$\begin{bmatrix} \delta h \\ \delta a \\ \delta b \end{bmatrix} = \delta C(\phi) B(\xi) \begin{bmatrix} h' \\ a' \\ b' \end{bmatrix} + C(\phi) \delta B(\xi) \begin{bmatrix} h' \\ a' \\ b' \end{bmatrix} + C(\phi) B(\xi) \begin{bmatrix} \delta h' \\ \delta a' \\ \delta b' \end{bmatrix} \quad (A-1)$$

where

$$\delta C = \delta c_{ij} = \begin{bmatrix} (-\sin \phi \delta \phi) & (-\cos \phi \delta \phi) & 0 \\ (\cos \phi \delta \phi) & (-\sin \phi \delta \phi) & 0 \\ 0 & 0 & 0 \end{bmatrix} = \begin{bmatrix} -\sin \phi & -\cos \phi & 0 \\ \cos \phi & -\sin \phi & 0 \\ 0 & 0 & 0 \end{bmatrix} \delta \phi = C^1 \delta \phi \quad (A-2)$$

and

$$\delta B = \delta b_{ij} = \begin{bmatrix} (-\sin \xi \delta \xi) & 0 & (\cos \xi \delta \xi) \\ 0 & 0 & 0 \\ (-\cos \xi \delta \xi) & 0 & (-\sin \xi \delta \xi) \end{bmatrix} = \begin{bmatrix} (-\sin \xi) & 0 & (\cos \xi) \\ 0 & 0 & 0 \\ (-\cos \xi) & 0 & (-\sin \xi) \end{bmatrix} \delta \xi = B^1 \delta \xi \quad (A-3)$$

For stereo angles,

$$\begin{bmatrix} \delta h' \\ \delta a' \\ \delta b' \end{bmatrix} = G_a(\alpha, \beta, \theta, L) \begin{bmatrix} \delta \alpha \\ \delta \beta \\ \delta \theta \\ \delta L \end{bmatrix} \quad (A-4)$$

where  $G_a$  is shown in Eq. (12b) in the text. The matrix  $G_a$  is obtained by taking the differentials of Eqs. (1a-c) with respect to  $\alpha, \beta, \theta$  and  $L$ .

For stereo range,

$$\begin{bmatrix} \delta h' \\ \delta a' \\ \delta b' \end{bmatrix} = G_r(M, N, K, L, J) \begin{bmatrix} \delta M \\ \delta N \\ \delta K \\ \delta L \\ \delta J \end{bmatrix} \quad (A-5)$$

where  $G_r$  is given in Eq. (13b) in the text. The matrix  $G_r$  is obtained from the differentials of Eqs. (4a-c) with respect to  $M, N, K, L$ , and  $J$ .

Equations (A-2), (A-3) and (A-4) are substituted into (A-1) to obtain:

$$\begin{bmatrix} \delta h \\ \delta a \\ \delta b \end{bmatrix} = \left\{ C^1(\phi)B(\xi) \begin{bmatrix} h' \\ a' \\ b' \end{bmatrix} : C(\phi)B^1(\xi) \begin{bmatrix} h' \\ a' \\ b' \end{bmatrix} \right\} \begin{bmatrix} \delta\phi \\ \delta\xi \end{bmatrix} + C(\phi)B(\xi)G_a(\alpha, \rho, \theta, L) \begin{bmatrix} \delta\alpha \\ \delta\rho \\ \delta\theta \\ \delta L \end{bmatrix} \quad (A-6)$$

Similarly, substitution of (A-2), (A-3) and (A-5) into (A-1) produces

$$\begin{bmatrix} \delta h \\ \delta a \\ \delta b \end{bmatrix} = \left\{ C^1(\phi)B(\xi) \begin{bmatrix} h' \\ a' \\ b' \end{bmatrix} : C(\phi)B^1(\xi) \begin{bmatrix} h' \\ a' \\ b' \end{bmatrix} \right\} \begin{bmatrix} \delta\phi \\ \delta\xi \end{bmatrix} + C(\phi)B(\xi)G_r(M, N, K, L, J) \begin{bmatrix} \delta M \\ \delta N \\ \delta K \\ \delta L \\ \delta J \end{bmatrix} \quad (A-7)$$

Comparing the above with (12a) or (13a)

$$D(h', a', b', \phi, \xi) = \left\{ C^1(\phi)B(\xi) \begin{bmatrix} h' \\ a' \\ b' \end{bmatrix} : C(\phi)B^1(\xi) \begin{bmatrix} h' \\ a' \\ b' \end{bmatrix} \right\} \quad (A-8)$$

The first term on the right is determined from (A-2) and (2c)

$$\begin{aligned} C^1 B \begin{bmatrix} h' \\ a' \\ b' \end{bmatrix} &= \begin{bmatrix} -\sin\phi & -\cos\phi & 0 \\ \cos\phi & -\sin\phi & 0 \\ 0 & 0 & 0 \end{bmatrix} \begin{bmatrix} \cos\xi & 0 & \sin\xi \\ 0 & 1 & 0 \\ -\sin\xi & 0 & \cos\xi \end{bmatrix} \begin{bmatrix} h' \\ a' \\ b' \end{bmatrix} \\ &= \begin{bmatrix} -\sin\phi & -\cos\phi & 0 \\ \cos\phi & -\sin\phi & 0 \\ 0 & 0 & 0 \end{bmatrix} \begin{bmatrix} h'\cos\xi + b'\sin\xi \\ a' \\ -h'\sin\xi + b'\cos\xi \end{bmatrix} \\ &= \begin{bmatrix} -h'\sin\phi\cos\xi - b'\sin\phi\sin\xi - a'\cos\phi \\ h'\cos\phi\cos\xi + b'\cos\phi\sin\xi - a'\sin\phi \\ 0 \end{bmatrix} \quad (A-9) \end{aligned}$$

The second term of (A-8) is determined from (A-3) and (2b)

$$\begin{aligned} CR^1 \begin{bmatrix} h' \\ a' \\ b' \end{bmatrix} &= \begin{bmatrix} \cos\phi & -\sin\phi & 0 \\ \sin\phi & \cos\phi & 0 \\ 0 & 0 & 1 \end{bmatrix} \begin{bmatrix} -\sin\xi & 0 & \cos\xi \\ 0 & 0 & 0 \\ -\cos\xi & 0 & -\sin\xi \end{bmatrix} \begin{bmatrix} h' \\ a' \\ b' \end{bmatrix} \\ &= \begin{bmatrix} \cos\phi & -\sin\phi & 0 \\ \sin\phi & \cos\phi & 0 \\ 0 & 0 & 1 \end{bmatrix} \begin{bmatrix} -h'\sin\xi + b'\cos\xi \\ 0 \\ -h'\cos\xi - b'\sin\xi \end{bmatrix} \end{aligned}$$

$$= \begin{bmatrix} -h' \cos \phi \sin \xi & +b' \cos \phi \cos \xi \\ -h' \sin \phi \sin \xi & +b' \sin \phi \cos \xi \\ -h' \cos \xi & -b' \sin \xi \end{bmatrix} \quad (\text{A-10})$$

Substitution of (A-9) and (A-10) into (A-8) gives

$$D(h', a', b', \phi, \xi) = \begin{bmatrix} (-h' \sin \phi \cos \xi & -a' \cos \phi & -b' \sin \phi \sin \xi) \\ (h' \cos \phi \cos \xi & -a' \sin \phi & +b' \cos \phi \sin \xi) \\ 0 \\ (-h' \cos \phi \sin \xi & +b' \cos \phi \cos \xi) \\ (-h' \sin \phi \sin \xi & +b' \sin \phi \cos \xi) \\ (-h' \cos \xi & -b' \sin \xi) \end{bmatrix} \quad (\text{A-11})$$

## APPENDIX B

### Derivation of the Covariance Matrix of the Variables

Equation (12) is multiplied by its transpose to prove the result shown in Eq. (16)

$$\begin{aligned} \begin{bmatrix} \delta h \\ \delta a \\ \delta b \end{bmatrix} \begin{bmatrix} \delta h & \delta a & \delta b \end{bmatrix} &= \left\{ D \begin{bmatrix} \delta \phi \\ \delta \xi \end{bmatrix} + \text{CBG}_a \begin{bmatrix} \delta \alpha \\ \delta \rho \\ \delta \theta \\ \delta L \end{bmatrix} \right\} \left\{ D \begin{bmatrix} \delta \phi \\ \delta \xi \end{bmatrix} + \text{CBG}_a \begin{bmatrix} \delta \alpha \\ \delta \rho \\ \delta \theta \\ \delta L \end{bmatrix} \right\}^T \\ &= D \begin{bmatrix} \delta \phi \\ \delta \xi \end{bmatrix} \begin{bmatrix} \delta \phi & \delta \xi \end{bmatrix} D^T + \text{CBG}_a \begin{bmatrix} \delta \alpha \\ \delta \rho \\ \delta \theta \\ \delta L \end{bmatrix} \begin{bmatrix} \delta \alpha & \delta \rho & \delta \theta & \delta L \end{bmatrix} G_a^T B^T C^T \\ &\quad + \text{CBG}_a \begin{bmatrix} \delta \alpha \\ \delta \rho \\ \delta \theta \\ \delta L \end{bmatrix} \begin{bmatrix} \delta \phi & \delta \xi \end{bmatrix} D^T + D \begin{bmatrix} \delta \phi \\ \delta \xi \end{bmatrix} \begin{bmatrix} \delta \alpha & \delta \rho & \delta \theta & \delta L \end{bmatrix} G_a^T B^T C^T \end{aligned} \quad (\text{B-1})$$

Expected values of (B-1) are taken to obtain

$$Y_a = E \left\{ \begin{bmatrix} \delta h \\ \delta a \\ \delta b \end{bmatrix} \begin{bmatrix} \delta h & \delta a & \delta b \end{bmatrix} \right\} = D E \left\{ \begin{bmatrix} \delta \phi \\ \delta \xi \end{bmatrix} \begin{bmatrix} \delta \phi & \delta \xi \end{bmatrix} \right\} D^T + \text{CBG}_a E \left\{ \begin{bmatrix} \delta \alpha \\ \delta \rho \\ \delta \theta \\ \delta L \end{bmatrix} \begin{bmatrix} \delta \alpha & \delta \rho & \delta \theta & \delta L \end{bmatrix} \right\} G_a^T B^T C^T +$$

$$+CBG_a^T E \left\{ \begin{bmatrix} \delta\alpha \\ \delta\beta \\ \delta\theta \\ \delta L \end{bmatrix} \begin{bmatrix} \delta\phi \\ \delta\zeta \end{bmatrix} \right\} D^T + D E \left\{ \begin{bmatrix} \delta\phi \\ \delta\zeta \end{bmatrix} \begin{bmatrix} \delta\alpha \\ \delta\beta \\ \delta\theta \\ \delta L \end{bmatrix} \right\} G_a^T B^T C^T \quad (B-2)$$

Assuming that  $\delta\alpha, \delta\beta, \delta\theta, \delta L, \delta\phi$  and  $\delta\zeta$  are uncorrelated, the last two terms of (B-2) reduce to zero. Eq. (B-2) then becomes Eq. (16).

Similarly, Eq. (13) may be multiplied by its transpose to yield Eq. (17).

### APPENDIX C

#### Derivation of the Slope Covariances

to prove Eqs. (21) and (22), (18b-d) are substituted into Eq. (18a)

to obtain

$$\bar{h} + \delta h = (\bar{A} + \delta A)(\bar{x} + \delta x) = \bar{A}\bar{x} + \delta A\bar{x} + \bar{A}\delta x + \delta A\delta x \quad (C-1)$$

The second order term  $\delta A\delta x$  may be neglected. Since  $\bar{h} = \bar{A}\bar{x}$

Eq. (C-1) may be reduced to

$$\bar{A}\delta x = \delta h - \delta A\bar{x}$$

This relation is pre-multiplied by  $\bar{A}^T$  to obtain

$$\bar{A}^T \bar{A} \delta x = \bar{A}^T (\delta h - \delta A\bar{x})$$

Therefore the estimate of  $\delta x$  becomes

$$\hat{\delta x} = (\bar{A}^T \bar{A})^{-1} \bar{A}^T (\delta h - \delta A\bar{x}) = F(\delta h - \delta A\bar{x}) \quad (C-2)$$

This is equivalent to Eqs. (20) and (21)

The product of Eq. (C-2) and its transpose provides

$$\hat{\delta x} \hat{\delta x}^T = F(\delta h - \delta A\bar{x})(\delta h - \delta A\bar{x})^T F^T = F[\delta h \delta h^T - \delta A \delta h^T - \delta h (\delta A\bar{x})^T + \delta A\bar{x} (\delta A\bar{x})^T] F^T \quad (C-3)$$

Taking the expected value of Eq. (C-3) results in Eq.(22)

in the text.

Eq. (23) may be substituted, term by term, into Eq. (22)

$$E(\hat{\delta x} \hat{\delta x}^T) = E \left\{ \begin{bmatrix} \hat{\delta x}_1 \\ \hat{\delta x}_2 \\ \hat{\delta x}_3 \end{bmatrix} \begin{bmatrix} \hat{\delta x}_1 & \hat{\delta x}_2 & \hat{\delta x}_3 \end{bmatrix} \right\} \quad (C-4)$$

$$E(\delta h \delta h^T) = E \left\{ \begin{bmatrix} \delta h_1 \\ \vdots \\ \delta h_n \end{bmatrix} \begin{bmatrix} \delta h_1 & \dots & \delta h_n \end{bmatrix} \right\} = \begin{bmatrix} E(\delta h_1)^2 & E(\delta h_1 \delta h_2) & E(\delta h_1 \delta h_n) \\ E(\delta h_2 \delta h_1) & E(\delta h_2)^2 & E(\delta h_2 \delta h_n) \\ \vdots & \vdots & \vdots \\ E(\delta h_n \delta h_1) & E(\delta h_n \delta h_2) & \dots E(\delta h_n \delta h_n) \end{bmatrix} \quad (C-5)$$

The different measurement points are uncorrelated. Therefore, the off diagonal terms are equal to zero. Eq. (C-5) reduces to

$$E(\delta h \delta h^T) = \begin{bmatrix} E(\delta h_1)^2 & & 0 \\ & \ddots & \\ 0 & & E(\delta h_n)^2 \end{bmatrix} \quad (C-6)$$

Similarly;

$$E(\delta A x \delta h^T) = E \left\{ \begin{bmatrix} \delta a_1 \bar{x}_1 + \delta b_1 \bar{x}_2 \\ \vdots \\ \delta a_n \bar{x}_1 + \delta b_n \bar{x}_2 \end{bmatrix} \begin{bmatrix} \delta h_1 & \dots & \delta h_n \end{bmatrix} \right\} \\ = \begin{bmatrix} E(\delta a_1 \delta h_1) \bar{x}_1 + E(\delta b_1 \delta h_1) \bar{x}_2 & & 0 \\ 0 & \ddots & \\ & E(\delta a_n \delta h_n) \bar{x}_1 + E(\delta b_n \delta h_n) \bar{x}_2 & \end{bmatrix} \quad (C-7)$$

$$E[\delta h (\delta A x)^T] = E \left\{ \begin{bmatrix} \delta h_1 \\ \vdots \\ \delta h_n \end{bmatrix} \begin{bmatrix} (\delta a_1 \bar{x}_1 + \delta b_1 \bar{x}_2) & \dots & (\delta a_n \bar{x}_1 + \delta b_n \bar{x}_2) \end{bmatrix} \right\} \\ = \begin{bmatrix} E(\delta h_1 \delta a_1) \bar{x}_1 + E(\delta h_1 \delta b_1) \bar{x}_2 & & 0 \\ & \ddots & \\ 0 & & E(\delta h_n \delta a_n) \bar{x}_1 + E(\delta h_n \delta b_n) \bar{x}_2 \end{bmatrix} \quad (C-8)$$

$$\begin{aligned}
E[\delta_{Ax} \delta_{Ax}^T] &= E \left\{ \begin{bmatrix} \delta_{a_1} \bar{x}_1 + \delta_{b_1} \bar{x}_2 \\ \vdots \\ \delta_{a_n} \bar{x}_1 + \delta_{b_n} \bar{x}_2 \end{bmatrix} \begin{bmatrix} (\delta_{a_1} \bar{x}_1 + \delta_{b_1} \bar{x}_2) \dots (\delta_{a_n} \bar{x}_1 + \delta_{b_n} \bar{x}_2) \end{bmatrix} \right\} \\
&= \begin{bmatrix} E(\delta_{a_1})^2 \bar{x}_1^2 + 2E(\delta_{a_1} \delta_{b_1}) \bar{x}_1 \bar{x}_2 + E(\delta_{b_1})^2 \bar{x}_2^2 & 0 \\ \vdots & \vdots \\ 0 & E(\delta_{a_n})^2 \bar{x}_1^2 + 2E(\delta_{a_n} \delta_{b_n}) \bar{x}_1 \bar{x}_2 + E(\delta_{b_n})^2 \bar{x}_2^2 \end{bmatrix} \\
&\quad (C-9)
\end{aligned}$$

The expected values in Eqs. (C-5) through (C-9) are calculated from Eq. (16) or Eq. (17) in the text.